AEDC-TR-71-143

FLOW FLUCTUATION MEASUREMENTS AT MACH NUMBER 4 IN THE TEST SECTION OF THE 12-INCH SUPERSONIC TUNNEL (D)

J. C. Donaldson and J. P. Wallace

ARO, Inc.

August 1971

Approved for public release; distribution unlimited.

VON KÁRMÁN GAS DYNAMICS FACILITY
ARNOLD ENGINEERING DEVELOPMENT CENTER
AIR FORCE SYSTEMS COMMAND
ARNOLD AIR FORCE STATION, TENNESSEE

69

NOTICES

When U. S. Government drawings specifications, or other data are used for any purpose other than a definitely related Government procurement operation, the Government thereby incurs no responsibility nor any obligation whatsoever, and the fact that the Government may have formulated, furnished, or in any way supplied the said drawings, specifications, or other data, is not to be regarded by implication or otherwise, or in any manner licensing the holder or any other person or corporation, or conveying any rights or permission to manufacture, use, or sell any patented invention that may in any way be related thereto.

Qualified users may obtain copies of this report from the Defense Documentation Center.

References to named commercial products in this report are not to be considered in any sense as an endorsement of the product by the United States Air Force or the Government.

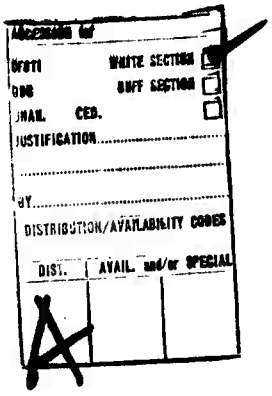

FLOW FLUCTUATION MEASUREMENTS AT MACH NUMBER 4 IN THE TEST SECTION OF THE 12-INCH SUPERSONIC TUNNEL (D)

J. C. Donaldson and J. P. Wallace
ARO, Inc.

FOREWORD

The work reported herein was sponsored by Headquarters, Arnold Engineering Development Center (AEDC), Air Force Systems Command (AFSC), Arnold Air Force Station, Tennessee, under Program Element 64719F. The work was done by ARO, Inc. (a subsidiary of Sverdrup & Parcel and Associates, Inc.), contract operator of AEDC under Contract F40600-72-C-0003. The experimental work was accomplished from June 25, 1969 to August 1, 1969, and the data analysis was completed on October 13, 1970. The ARO Project Number was VT8002, and the manuscript was submitted for publication on May 4, 1971.

The authors wish to acknowledge the assistance received in this investigation from the colleagues of the first author at the von Kármán Gas Dynamics Facility, AEDC. Appreciation is expressed specifically to M. D. Brown for his assistance in clarifying the instrumentation electronics and to J. H. Norman, Jr., for his patient preparation of the hot-wire anemometer probes. Special appreciation is also expressed to J. L. Welsh and his group at the Engine Test Facility, AEDC, for obtaining the power spectral density analyses of the hot-wire and microphone output signals.

Dr. J. P. Wallace, College of Engineering, Tennessee Technological University, served as a consultant to ARO, Inc.

This technical report has been reviewed and is approved.

Emmett A. Niblack, Jr.
Lt Colonel, USAF
AF Representative, VKF
Directorate of Test

Joseph R. Henry
Colonel, USAF
Director of Test

UNCLASSIFIED

Security Classification

DOCUMENT CONTROL DATA - R & D

(Security classification of title, body of abstract and indexing annotation must be entered when the overall report is classified)

1. ORIGINATING ACTIVITY *(Corporate author)*
Arnold Engineering Development Center, ARO, Inc., Operating Contractor, Arnold Air Force Station, Tennessee 37389

2a. REPORT SECURITY CLASSIFICATION
UNCLASSIFIED

2b. GROUP
N/A

3. REPORT TITLE
FLOW FLUCTUATION MEASUREMENTS AT MACH NUMBER 4 IN THE TEST SECTION OF THE 12-INCH SUPERSONIC TUNNEL (D)

4. DESCRIPTIVE NOTES *(Type of report and inclusive dates)*
June 25 to August 1, 1969--Final Report

5. AUTHOR(S) *(First name, middle initial, last name)*
J. C. Donaldson and J. P. Wallace, ARO, Inc.

6. REPORT DATE	7a. TOTAL NO. OF PAGES	7b. NO. OF REFS
August 1971	68	31

8a. CONTRACT OR GRANT NO.	9a. ORIGINATOR'S REPORT NUMBER(S)
F40600-72-C-0003	AEDC-TR-71-143
b. Program Element 64719F	
c.	9b. OTHER REPORT NO(S) *(Any other numbers that may be assigned this report)*
d.	ARO-VKF-TR-71-90

10. DISTRIBUTION STATEMENT
Approved for public release; distribution unlimited.

11. SUPPLEMENTARY NOTES	12. SPONSORING MILITARY ACTIVITY
Available in DDC.	Arnold Engineering Development Center, Arnold Air Force Station, Tennessee 37389

13. ABSTRACT

Hot-wire anemometry measurements were made in the 12-in. supersonic tunnel of the von Karman Gas Dynamics Facility to determine the level of flow fluctuations in the free stream. Supplementary acoustic measurements were made using a microphone mounted flush with the top surface of a flat plate. Data were obtained at Mach number 4. Reynolds number, based on the wire diameter (d = 0.0001 in.), ranged from 5.0 to 24.0. The hot-wire anemometry results presented are based on the mode concept of Kovasznay and the techniques of Morkovin for hot-wire data reduction. The free-stream results, which are similar to those published by Dr. John Laufer, can be explained by the assumption of a sound source traveling in the tunnel wall boundary layer at a supersonic velocity relative to the free stream. The acoustic measurements on the surface of the flat plate revealed pressure fluctuation levels larger than those of the free stream by a factor of at least 20.

DD FORM 1 NOV 68 1473

UNCLASSIFIED

Security Classification

14. KEY WORDS	LINK A		LINK B		LINK C	
	ROLE	WT	ROLE	WT	ROLE	WT
flow measurements						
hot-wire anemometers						
anemometers						
acoustic measurements						
supersonic flow						
Reynolds number						
test facilities						

ABSTRACT

Hot-wire anemometry measurements were made in the 12-in. supersonic tunnel of the von Kármán Gas Dynamics Facility to determine the level of flow fluctuations in the free stream. Supplementary acoustic measurements were made using a microphone mounted flush with the top surface of a flat plate. Data were obtained at Mach number 4. Reynolds number, based on the wire diameter (d = 0.0001 in.), ranged from 5.0 to 24.0. The hot-wire anemometry results presented are based on the mode concept of Kovasznay and the techniques of Morkovin for hot-wire data reduction. The free-stream results, which are similar to those published by Dr. John Laufer, can be explained by the assumption of a sound source traveling in the tunnel wall boundary layer at a supersonic velocity relative to the free stream. The accustic measurements on the surface of the flat plate revealed pressure fluctuation levels larger than those of the free stream by a factor of at least 20.

CONTENTS

APPENDIXES

I. ILLUSTRATIONS

Figure

NOMENCLATURE

A'_w	Overheating parameter, $1/2\,(\partial \ell n\, R_w/\partial \ell n\, I)_h$
a	Velocity of sound, ft/sec
a'_w	Overheating parameter, $(R_w - R_r)/R_r$
$\bar{b}$	Average value of flat plate leading-edge thickness, in.
C_T	Thermal capacity of wire, Btu/°R
d	Wire diameter, in.
E	Thermal energy accumulated in wire, Btu
E_e	Energy density distribution function of mean-square wire voltage output, v^2/Hz
E'	Finite circuit parameter
e	Voltage across wire, v
Δe	Instantaneous change of voltage from mean, v
$\Delta e_{(\ )}$	Sensitivity coefficient for component indicated by subscript, v
$F_{(\ )}$	Energy density distribution function of the quantity indicated by the subscript, v^2/Hz
f	Frequency, Hz
Δf	Frequency band, Hz
G	Normalized energy density distribution function, $(Hz)^{-1}$
H	Rate of heat loss of wire, Btu/sec
h	Convective heat-transfer coefficient, $H/\pi d\ell(T_w - T_r)$, Btu/ft^2 sec °R
I	Mean wire current, amp
K	$\partial \ell n\, R_w/\partial \ell n\, T_w$
k_o	Heat conductivity for air at T_o, Btu/ft sec °R

ℓ	Wire length, in.
M	Mach number
τ	Time constant of hot wire, sec
m	Mass flow, $lbm/ft^2 sec$
Δm	Fluctuating component of mass flow, $lbm/ft^2 sec$
Nu_o	Nusselt number, $h\,d/k_o$
n_x	Direction cosine of normal to sound plane wave front relative to flow direction
p	Local static pressure, psia
Δp	Fluctuating component of pressure, psi
p_o	Tunnel stilling chamber stagnation pressure, psia
q	Dynamic pressure, psia
Re/in.	Unit Reynolds number based on free-stream conditions, $\rho_\infty u_\infty/\mu_\infty$
Re_o	Reynolds number of wire, $\rho_\infty u_\infty\, d/\mu_o$
$R_{(\ )}$	Resistance of wire at condition indicated by subscript, ohm
$R_{(\ )(\ )}$	Correlation coefficient for components indicated by subscripts
s	Standard deviation
T	Static temperature, °R
ΔT_o	Fluctuating component of stagnation temperature, °R
T_o	Stagnation temperature (measured in tunnel stilling chamber), °R
T_2	Static temperature behind a normal shock wave, °R
$T_{(\ )}$	Temperature of wire at condition indicated by subscript, °R
t	Time, sec
u	Velocity in mean flow direction, ft/sec
Δu	Fluctuating component of velocity, ft/sec
Δu_n	Fluctuating component of particle velocity normal to sound wave, ft/sec
u_r	Velocity of free stream relative to sound source velocity u_s, ft/sec

u_s	Velocity of sound source, ft/sec
W	Thermal energy generated in wire per unit time, Btu/sec
X	Overheating parameter, $\Delta e_\tau / \Delta e_\sigma$
Y	Nondimensional rms voltage fluctuation, $\tilde{e}/\Delta e_\sigma$
α	Temperature linear coefficient of resistivity, $(°R)^{-1}$
α_M	$\left[1 + 0.5\,(\gamma-1)M^2\right]^{-1}$
β	Temperature non-linear coefficient of resistivity, $(°R)^{-2}$
β_M	$\alpha_M(\gamma-1)M^2$
γ	Ratio of specific heats, 1.40
δ	Thickness of tunnel wall boundary layer
η	Temperature recovery factor of wire (I = 0), T_r/T_o
θ	Angle between the flow direction and the normal to the sound plane wave front, deg
θ_{LE}	Bevel angle of flat plate leading edge, deg
λ	Wavelength of sound field
μ	Viscosity, lbm/ft sec
π	Sound mode "amplitude"
$\pi(f)$	Sound energy density at frequency f
ρ	Density, lbm/ft^3
$\Delta\rho$	Fluctuating component of density, lbm/ft^3
σ	Entropy mode "amplitude"
τ	Vorticity mode "amplitude"
τ_r	Temperature loading, $(T_w - T_r)/T_r$
τ_w	Average wall shearing stress, psi
ϕ	Roll angle, positive for clockwise rotation, deg

SUBSCRIPTS

e	Pertaining to voltage response
f	Pertaining to reference temperature of 32°F
h	Controlled heating of wire while rest of system, including flow parameters, is constant

m	Pertaining to mass flow
o	Stagnation condition
p	Pertaining to pressure
r	Pertaining to temperature of unheated wire (I = 0)
T	Pertaining to stagnation temperature
u	Pertaining to velocity
w	Pertaining to temperature of heated wire
∞	Free-stream condition
π	Pertaining to sound mode
ρ	Pertaining to density
σ	Pertaining to entropy mode
τ	Pertaining to vorticity mode

SUPERSCRIPTS

$(\tilde{})$	Root mean square (rms) value of a fluctuating quantity
$(\bar{})$	Average with respect to time

SECTION I
INTRODUCTION

The fluctuating variables in the free stream of a supersonic wind tunnel test section have been accorded much interest by investigators of such allied phenomena as boundary-layer transition, flow separation, boundary-layer control, heat transfer, etc. However, few measurements of supersonic flow fluctuations have been published. As consideration is given to the importance of high-speed turbulence and related factors in the design and performance of new vehicles, the capability of measuring flow fluctuations may become a requirement of wind tunnel test facilities. The capability of determining flow fluctuations in a wind tunnel is desirable from two points of view: the intrinsic relation of the fluctuating quantities to phenomena investigated in wind tunnel testing and the inherent role of the fluctuations in the correlation of phenomena among various wind tunnels.

Kovasznay (Ref. 1) has shown that the random fluctuations in a supersonic flow are composed of three types or modes of disturbance: the vorticity, entropy, and sound-wave modes. Morkovin (Ref. 2) has discussed the possible sources of the different modes. Briefly, Morkovin has reasoned that the vorticity and entropy fluctuations in the free stream have their origins in the tunnel settling chamber or upstream, and that the sound fluctuations are generated within the boundary layers on the tunnel walls. Morkovin points out that vorticity (turbulent velocity) fluctuations are effectively suppressed by a large speed ratio across the nozzle. He also comments that the decay of entropy fluctuations (temperature spottiness) is accelerated by mixing upstream of the settling chamber and by screens in the settling chamber. It is concluded that the magnitude of free-stream vorticity and entropy fluctuations in the supersonic test section are to a large extent subject to control. On the other hand, it does not appear that design considerations can greatly alter the level of the sound mode of fluctuations in the free stream.

Some years ago (in 1954) the importance of pressure fluctuations (sound) emanating from turbulent boundary layers on the walls of supersonic wind tunnels was suggested by Laufer (Ref. 3). Subsequent work by Laufer (Refs. 4 and 5), using hot-wire anemometry techniques, established the level of sound fluctuations in the free stream of one wind tunnel. More recently the influence of aerodynamic noise radiated from tunnel wall boundary layers upon transition of the boundary layer of test models has been investigated by Pate and Schueler (Ref. 6).

The present report presents results of measurements of the fluctuating variables in the free-stream flow field of one of the supersonic wind tunnels (Tunnel D) of the von Kármán Gas Dynamics Facility (VKF) used in Pate and Schueler's studies. In conjunction with these measurements, it has been the objective of this investigation to develop a capability within the VKF to use the hot-wire anemometer as a measurement tool in high-speed flows. Although the heated fine wire is not a convenient device to use and the associated data analysis cannot be called routine, the small size of the measuring element and the ability of the heated wire with its associated electrical equipment to respond to high frequency fluctuations make the hot-wire anemometer the principal instrument now in use for studying high-speed flow fluctuations.

Hot-wire measurements were made at Mach number 4 at three unit Reynolds numbers: 0.05, 0.12, and 0.24 million per inch. Supplementary measurements were made using a microphone mounted on a flat plate.

SECTION II
APPARATUS

2.1 WIND TUNNEL

Tunnel D is an intermittent, variable density wind tunnel with a manually adjusted, flexible plate-type nozzle and a 12- by 12-in. test section. The tunnel can be operated at Mach numbers from 1.5 to 5 at stagnation pressures from about 3 to 60 psia and at an average stagnation temperature of about 70°F. A description of the tunnel and airflow calibration information may be found in Ref. 7. An illustration showing the Tunnel D geometry is presented in Fig. 1 (Appendix I). It is of interest to note that Tunnel D is a modified copy of the 12-in. supersonic wind tunnel which was previously in operation at the Jet Propulsion Laboratory, California Institute of Technology.

The hot-wire measurements of the present investigation were made on the centerline of the tunnel at the centerline of the viewing windows or approximately 55.1 in. downstream of the throat. At this location each of the boundary layers of the tunnel walls is approximately 1.0 to 1.5 in. thick, depending on the free-stream unit Reynolds number (Ref. 7).

For Mach number 4, the contraction ratio upstream of the Tunnel D nozzle throat, that is the cross-sectional area of the stilling chamber divided by the area of the throat, is approximately 84 to 1.

2.2 HOT-WIRE PROBES

The hot-wire probes used in this investigation (Fig. 2) were fabricated by the VKF and were similar in design to probes used successfully in supersonic flow by Laufer and Vrebalovich (Refs. 4, 8, and 9). Needles were glued to a razor blade section attached to a mounting strut. The needles extended 0.04 in. upstream of the leading edge of the blade, with a nominal spacing of 0.015 in. at the tips. Probes of a different design, with needles extending 0.7 in., which were used in earlier VKF hot-wire measurements in low density separated flow, were tried initially in the present case, but the wire supports were not sufficiently stable relative to one another so that the wires on these probes failed upon exposure to the free stream.

Platinum-10 percent rhodium wire drawn by the Wollaston process was used for the sensing element of the hot-wire probes. The silver sleeve of the Wollaston process which surrounded the fine wire was removed by etching in nitric acid using a small electric de-plating current. After removing the sleeve, the wire was soft-soldered to the probe needles, leaving slack to reduce tension in the wire under loading (see Fig. 2c). Each wire was annealed by heating it in still air for approximately five minutes.

The manufacturer's nominal value for the wire diameter ($d = 1.0 \times 10^{-4}$ in.) was accepted for the data reduction. According to the manufacturer, the wire was drawn to a resistance tolerance of ±5 percent, not to a diameter measurement tolerance. A value for the resistivity of the annealed platinum-10 percent rhodium wire (111 ohms per circular mil foot) was obtained from the manufacturer and was used to calculate the length of each wire from the measured resistance. The two probes used for the measurements had wire aspect ratios (ℓ/d) of approximately 140 and 160.

The relationship between the resistance and temperature of a heated fine wire may be stated by the equation:

$$R_w = R_f\left[1 + \alpha_f(T_w - T_f) + \beta_f(T_w - T_f)^2\right]$$

where the subscript w refers to the heated conditions and the subscript f to the chosen reference conditions. A sample of the wire used in the present measurements was check-calibrated against the nominal value for α_f obtained from Morkovin (Ref. 10) ($\alpha_f = 8.9 \times 10^{-4}$ per °R for $T_f = 492$°R). The nominal value was acceptable within the estimated uncertainties of the calibration. The value for β_f obtained from Morkovin

(nominal β_f = -4.8 x 10^{-8} per °R^2) was of negligible significance for the range of applicable temperatures encountered in the present study.

2.3 MICROPHONE

Supplementary pressure fluctuation measurements were made using Brüel and Kjaer, Model No. 4136, 0.25-in.-diam condenser microphone cartridge mounted in a flat plate, as shown in Fig. 3. The microphone system consisted of the following Brüel and Kjaer components connected to the cartridge: a flexible adapter, type UA0122; a cathode follower, type 2615; and the power supply, type 2801. The system had a flat (±2 decibel (db)) frequency response at atmospheric pressure from 30 Hz to 70 kHz and a dynamic pressure range of from 70 to 180 db, referenced to a sound pressure of 0.0002 microbar. The sensitivity of the microphone system in terms of output voltage to applied pressures was determined by VKF calibration to be 0.070 millivolt/microbar.

The flat-plate model was designed to accommodate a second microphone mounted internally (Fig. 3) to monitor the effects of model vibration on microphone response. Inasmuch as these effects had previously been found negligible (Ref. 6) under similar test conditions, the second microphone was omitted from the present study. The air mass within the condenser microphone provides mechanical damping for the microphone diaphragm. Design considerations make the damping critical at an ambient pressure of one atmosphere, in order to give the widest frequency range of flat response to sound pressure fluctuation at that condition. When the microphone is operated in an environment of subatmospheric pressure, the frequency response is altered, especially at the higher frequencies, by a resonance peak, and the output signals which are centered about the resonance frequency (45 kHz in the present case) introduce errors into the sound pressure measurements. For present purposes, however, the resonance contribution was determined by playback of the tape-recorded microphone output through a Spencer-Kennedy Model 302 variable electronic bandpass filter set to pass signals from 45 to 55 kHz. (The attenuation at the filter cutoff frequencies was 1.8 db with a rejection rate of 18 db per octave, according to the manufacturer's specifications.) The mean-square of the resonance contribution was read, using the true rms meter, for each measurement, and the result was then subtracted from the mean-square of the total microphone output.

2.4 HOT-WIRE AND MICROPHONE INSTRUMENTATION

The hot-wire anemometer measurements were made using commercially available constant-current equipment (Fig. 4) of Shapiro and Edwards design (Model 50).

The amplifier (Model A-50C) has a design frequency range of from 1 Hz to 320 kHz. Coupling circuits are provided within the amplifier to permit control of the low frequency and high frequency cut-off characteristics. The amplifier has a maximum gain of 50, 000 between input and output, with the compensation network off. Maximum gain when fully compensated is 2.5×10^6. The gain of the amplifier is variable over a range of 1028:1 in 21 steps of 0.707:1 ± 1 percent (approximately 3 db) each. The maximum uncompensated gain was checked at least once each day of operation.

A compensating network is incorporated in the amplifier to offset the effect of the thermal inertia of the hot-wire at higher frequencies. The network is capable of compensating wires with time constants between 0.05 and 22.0 msec. The ratio between basic amplification and the maximum amplification of the compensating circuit is 500 for any setting of the time constant.

Wire-heating currents can be adjusted over the range of from 1 to 300 ma. The current was measured using a precision potentiometer with ranges of 1.0, 0.1, and 0.01 amp full scale with a precision of ±0.1 percent of full scale.

The resistance of the wire was measured using a precision bridge with a precision of ±0.01 ohms or ±0.05 percent of the reading, whichever is greater.

The ratio of signal-to-noise was improved by using an input transformer which increased the input signal voltage to the amplifier by a factor of five. The transformer has two frequency ranges: 25 Hz to 40 kHz and 1 kHz to 320 kHz. In the present investigation, data were obtained for both ranges.

The rms voltage fluctuations of the wire were fed from the amplifier to a Brüel and Kjaer true-rms meter, type 2409. Each reading (which had an uncertainty of ±2.0 percent) was corrected for amplifier electronic noise determined for the individual control settings of the amplifier. Microphone output was measured using the same meter.

Magnetic tape recordings of the hot-wire anemometer amplifier output were made using an Ampex Model FR 1300 analog tape recorder. The hot-wire signals were recorded simultaneously on a direct channel and an FM channel having frequency responses from 300 Hz to 300 kHz and dc to 20 kHz, respectively. Signals from the microphone on the flat plate were recorded for tunnel flow conditions which duplicated (on separate runs) those for the hot-wire data. Microphone signals were recorded only on a direct channel.

Power spectra of the hot-wire response signals and of the microphone signals were determined using a Honeywell 9300 automatic wave analyzer system. This system is designed to analyze signals in the frequency range from 2 Hz to 40 kHz. Available analysis bandwidths are 1, 5, 10, and 50 Hz. The analysis of signals of higher-frequency content may be obtained through tape playback speed reduction. In the present case, selected hot-wire signals were analyzed to give power spectra over the frequency range from 20 Hz to 120 kHz.

SECTION III
DISCUSSION OF HOT WIRE MEASUREMENTS

3.1 DATA ACQUISITION AND REDUCTION CONSIDERATIONS

The analysis of the structure of turbulence in a compressible, viscous, heat-conductive gas by perturbation techniques has been reported by Kovasznay (Ref. 1) and Chu and Kovasznay (Ref. 11). Kovasznay's linearized analysis (Ref. 1) identified three types or modes of fluctuations: vorticity, entropy, and sound. In that analysis the three modes are treated as completely decoupled; that is, energy transfer from one mode to another is not allowed. Chu and Kovasznay (Ref. 11) generalized the analysis to include interactions between modes in the form of bilateral (second-order) terms. Fortunately, in a small space-time domain without solid boundaries, such as the close neighborhood of a fine heated wire, the interactions are of a weak nature, and therefore, may be neglected. The concepts of Refs. 1 and 11 serve as a basis for the interpretation of the fluctuation measurements made using the hot-wire anemometer.

The basic relation for the response of the hot wire, immersed in a flow field, and the associated electrical system to fluctuations of the flow is stated as follows:

$$\Delta e + \mathfrak{M}\frac{d\Delta e}{dt} = -\Delta e_{\rho}\left(\frac{\Delta\rho}{\bar{\rho}}\right) - \Delta e_{u}\left(\frac{\Delta u}{\bar{u}}\right) + \Delta e_{T}\left(\frac{\Delta T_{o}}{\bar{T}_{o}}\right)$$

where Δe is the instantaneous voltage change from the mean voltage drop $\bar{e}$ across the wire; $\mathbb{M}$ is the time constant of the wire; t is time; $\Delta\rho$, Δu, ΔT_o are the fluctuating components of the mean flow density $\bar{\rho}$, velocity $\bar{u}$, and total (stagnation) temperature $\bar{T}_o$, respectively; and Δe_ρ, Δe_u, and Δe_T are the sensitivity coefficients of the heated wire. The time constant and the sensitivity coefficients are dependent on the properties of the wire, of the electrical system, and of the mean flow. The second term on the left side of the equation is effectively made to vanish by proper compensation, within the electrical system, for the thermal inertia of the wire.

In order to infer flow fluctuation quantities, the sensitivity coefficients must be evaluated either through a calibration technique where flow conditions are known or by relating the heat-transfer characteristics of the wire to the electrical circuit parameters through empirical correlations. The latter technique is most often used because of the short life-expectancy of a given wire. Consideration will now be given to the derivation of expressions for the sensitivity coefficients.

The energy balance for the heated wire without end losses, averaged over the length of the wire, is simply stated by the equation

$$dE/dt = W - H$$

where E is the heat stored in the wire, W represents the thermal energy generated in the wire per unit time, and H represents the rate of heat loss to the fluid flowing around the wire. The heat stored in a wire, $E = C_T T_w$, at temperature T_w is viewed as constant when the wire is properly compensated for thermal lag resulting from the finite heat capacity C_T of the wire. The power

$$W = JI^2 R_w = JI^2 R_f[1 + \alpha_f(T_w - T_f) + \beta_f(T_w - T_f)^2]$$

is generated by the heating current I, but W also depends on the temperature T_w of the wire relative to a reference temperature T_f and on the calibration of the wire which yields the constants R_f, α_f, and β_f (J is a units conversion factor). The heat loss $H = Nu_o \pi \ell k_o(T_w - T_r)$ is stated in terms of the Nusselt number $Nu_o = h\, d/k_o$ and the "equilibrium" or recovery temperature $T_r = \eta T_o$ of the unheated wire.

In order to relate the heat loss of a hot wire to the conditions of the flow, it is necessary to know the steady-state heat loss relationship applicable to the given flow field. Such relationships are usually stated in terms of the Nusselt number (Nu_o) as a function of Mach number (M_∞) and Reynolds number ($Re_o = \rho_\infty u_\infty d/\mu_o$) where the air thermal

conductivity k_o and viscosity μ_o are based on the stagnation temperature.[1] In supersonic flow, this reference temperature has the advantages of remaining unchanged across shock waves and of being a good approximation for the free-stream temperature (T_2) behind a normal shock wave (or an almost-normal wave, such as the shock wave immediately upstream of the blunt wire). This fact becomes particularly advantageous when it is realized (Ref. 12) that flow conditions behind the detached shock wave and in the vicinity of the wire are only weakly dependent on the free-stream Mach number. Further, when calculating the energy loss from the wire, it is necessary to know the functional dependence of the temperature recovery factor (η) on the relevant flow parameters.

The required relations can be obtained by calibrating the wire in the flow field to be investigated. It should be noted that this calibration is concerned with mean values of the variables, not with fluctuations. Alternatively, quantitative results can be obtained at the sacrifice of some accuracy by reliance on existing correlation functions (Refs. 9 and 10). Relationships have been established for infinite-length wires as a result of the work of many investigators and have been formulated empirically for wide ranges of Mach number and Reynolds number by Dewey (Ref. 13) and others. In the present investigations empirical relations were used in lieu of direct calibration of each wire because of the short life-expectancy of a fine wire in supersonic flow. For simplicity, the data of the present investigation have been reduced using information presented by Vrebalovich (Ref. 9), who has expressed Nusselt number for (infinite-length) wires in supersonic flow ($M \geq 1.2$) as a function of Reynolds number only and has presented a table of experimental data relating the recovery temperature factor to Reynolds number only (see Fig. 5).

Thermal lag due to the finite heat capacity of a wire causes the response of the heated wire to flow fluctuations to decrease at higher frequencies. The compensation network within the anemometer amplifier circuit permits electrical compensation for the thermal inertia of the heated wire; that is, the response of the amplifier is made to increase at higher frequencies. As a consequence, however, electronic

---

[1] In the general case of heat transfer from an infinite-length wire, the Nusselt number is a function of Reynolds number, Mach number, and temperature loading (τ_r) for a given gas, with constant Prandtl number and constant ratio of specific heats (γ). The experiments of Laufer and McClellan (Ref. 12) have shown that the temperature loading is a weak parameter and that the slope of the Nusselt number versus Reynolds number correlation varies only slightly over a wide range of temperature loadings.

noise is also amplified, and the signal-to-noise ratio decreases. To minimize the thermal lag and obtain a useful signal-to-noise ratio, the diameter and length of the wire must be quite small. It must be noted, however, that in order to obtain correct high frequency response it is necessary to minimize temperature gradients along the wire by requiring a large length-to-diameter ratio. The availability of an input transformer to boost the strength of the signal from the wire was found to be valuable in obtaining reasonable signal-to-noise ratios for the supersonic flow field of the present study.

The time constant for thermal lag compensation was determined for each data point by the square-wave technique (Ref. 14). Some uncertainty is associated with this method of experimental time constant determination because of the superposed turbulence signal and amplifier noise. The computational schemes of Morkovin and Phinney (Ref. 15) and Vrebalovich (Ref. 9) were used to minimize the uncertainties. Morkovin and Phinney (Ref. 15) show that the ratio of the time constant of the correct compensation setting to that of an incorrect setting is equal to the ratio of the correct value of the rms voltage output to the incorrect value, provided that the energy density contribution to the overall signal of the uncompensated wire is small. The difficulty with this correction procedure lies in determining the "correct" time constant value. To overcome this difficulty, Vrebalovich suggests (Ref. 9) calculating the heat capacity (C_T) of the wire for each point in a set of data, obtaining the average heat capacity ($\bar{C}_T$) for the set, and assuming the average value to be the "correct" value. The "correct" time constant is then calculated from $\bar{C}_T$ and applied in the correction technique of Morkovin and Phinney (Ref. 15). Discussion of the effect of this correction will be deferred until a later section of this report.

Inasmuch as the electric circuit which supplies current to heat the wire of the "constant-current" anemometer has a finite impedance, the current is not truly constant when the wire resistance is made to vary by fluctuations in the flow. The variations in the voltage (e) and thermal energy (W) are small, but they must be taken into account using a finite-circuit parameter in the equation for the conservation of heat.

The factors discussed above which are related to the heat balance of the hot wire have been considered by Morkovin (Ref. 10) in obtaining expressions for the sensitivity coefficients. Assuming proper compensation so that $dE/dt = 0$ and introducing small perturbations into the steady-state energy equation ($W = H$) in logarithmic form, Morkovin derived the following expressions:

$$\Delta e_\rho = \bar{\varepsilon} E' A'_w \left[\frac{\partial \ell n \, Nu_o}{\partial \ell n \, Re_o} - \frac{1}{r_r} \frac{\partial \ell n \, \eta}{\partial \ell n \, Re_o} \right]$$

$$\Delta e_u = \Delta e_\rho + \bar{\varepsilon} E' \left(\frac{A'_w}{a_M} \right) \left[\frac{\partial \ell n \, Nu_o}{\partial \ell n \, M} - \frac{1}{r_r} \frac{\partial \ell n \, \eta}{\partial \ell n \, M} \right]$$

$$\Delta e_T = \bar{\varepsilon} E' \left[K + A'_w \left(K - 1.885 + 0.765 \frac{\partial \ell n \, Nu_o}{\partial \ell n \, Re_o} + \frac{0.5}{a_M} \frac{\partial \ell n \, Nu_o}{\partial \ell n \, M} \right) - \frac{A'_w}{r_r} \left(0.765 \frac{\partial \ell n \, \eta}{\partial \ell n \, Re_o} + \frac{0.5}{a_M} \frac{\partial \ell n \, \eta}{\partial \ell n \, M} \right) \right]$$

where E' is a finite-circuit parameter and where $A'_w = 0.5 \, (\partial \ell n \, R_w / \partial \ell n I)_h$ is the local logarithmic slope of the resistance-current variation and the subscript h specifies controlled heating of the wire while the rest of the system, including the flow parameters, are maintained constant. Inasmuch as the wire resistance may vary with wire location in the flow-field as well as with the heating current, the slope A'_w must be determined at each operating point, leading to the description by Morkovin (Ref. 16) of A'_w as a "locally linearized, locally calibrated overheat parameter."

The various logarithmic derivatives which appear explicitly in the above equations for the sensitivity coefficients are determined from the relations for Nusselt number and temperature recovery factor obtained by calibration or through use of the correlations. It must be pointed out here that a significant portion of the heat generated in the hot wire is conducted to the cooler wire support needles, indicating a higher experimental Nusselt number than actually exists. For this reason, corrections for heat-loss to the needles are required in calculating finite-length wire sensitivity coefficients. Specifically, logarithmic derivatives determined from correlations written for wires of infinite length must be "corrected" for use with measurements made with real wires. The method usually used (Refs. 9 and 10) to account for end conduction losses, and used in the present investigation, was developed by Kovasznay and Tornmarck (Ref. 17) and again presented in detail by Kovasznay in Ref. 14. End-loss correction is not required with wires which have been individually calibrated.

When the wire Nusselt number and temperature recovery factor are independent of Mach number, as in supersonic flow fields, the wire sensitivity coefficients for density and velocity are equal:

$$\Delta e_\rho = \Delta e_u = \Delta e_m$$

where Δe_m is the sensitivity to mass flow fluctuations. The basic equation for the response of a properly compensated hot wire is

$$\Delta e = -\Delta e_\rho \left(\frac{\Delta \rho}{\bar{\rho}} \right) - \Delta e_u \left(\frac{\Delta u}{\bar{u}} \right) + \Delta e_T \left(\frac{\Delta T_o}{\bar{T}_o} \right)$$

becomes, then, for a supersonic flow field,

$$\Delta e = -\Delta e_m\left(\frac{\Delta m}{\bar{m}}\right) + \Delta e_T\left(\frac{\Delta T_o}{\bar{T}_o}\right)$$

with mass flow fluctuations,

$$\frac{\Delta m}{\bar{m}} = \left(\frac{\Delta \rho}{\bar{\rho}}\right) + \left(\frac{\Delta u}{\bar{u}}\right)$$

and total temperature fluctuations,

$$\frac{\Delta T_o}{\bar{T}_o} = a_M\left(\frac{\Delta T}{\bar{T}}\right) + \beta_M\left(\frac{\Delta u}{\bar{u}}\right)$$

The mean-square of the voltage fluctuation output of the heated wire is given by

$$\overline{(\Delta e)^2} = (\tilde{e})^2 = (\Delta e_m)^2\left(\frac{\tilde{m}}{\bar{m}}\right)^2 + (\Delta e_T)^2\left(\frac{\tilde{T}_o}{\bar{T}_o}\right)^2 - 2\,\Delta e_m\,\Delta e_T\left(\frac{\tilde{m}}{\bar{m}}\right)\left(\frac{\tilde{T}_o}{\bar{T}_o}\right) R_{mT}$$

where the tilde ($\sim$) indicates an rms fluctuation and

$$R_{mT} = \frac{\overline{(\Delta m)(\Delta T_o)}}{\tilde{m}\,\tilde{T}_o}$$

is the correlation coefficient. Measurements made at three distinct wire heating currents will yield three equations for simultaneous solution for the three unknowns ($\tilde{m}$, $\tilde{T}_o$, and R_{mT}), but uncertainties in the measurements are likely to produce scatter in the results. The effects of the uncertainties can be minimized by using a greater number of measurements and a graphical solution for the unknowns. This manner of presentation of hot-wire data was introduced by Kovasznay (Ref. 1) for supersonic flow-field measurements and involves only the rewriting of the basic equation in the form:

$$\frac{\tilde{e}^2}{(\Delta e_T)^2} = \left(\frac{\Delta e_m}{\Delta e_T}\right)^2\left(\frac{\tilde{m}}{\bar{m}}\right)^2 - 2\left(\frac{\Delta e_m}{\Delta e_T}\right)\left(\frac{\tilde{m}}{\bar{m}}\right)\left(\frac{\tilde{T}_o}{\bar{T}_o}\right) R_{mT} + \left(\frac{\tilde{T}_o}{\bar{T}_o}\right)^2$$

and the determination of values for the coefficients which give the best curve among the measurements plotted in the form of ($\tilde{e}/\Delta e_T$) versus ($\Delta e_m/\Delta e_T$). Further discussion of the use of the Kovasznay-type of mode diagram will be found in Section 3.2.

While the wire responds to fluctuations of the density, velocity, and temperature, the independent fluctuations which characterize the turbulent flow field are the vorticity (turbulence), entropy (temperature spottiness), and sound modes. These modes are related to the density,

velocity, and total-temperature sensitivity coefficients given above by the following expressions (Ref. 11) [the expanded equations are given in Table I (Appendix II)]:

$$\Delta e_\tau = -\Delta e_u + \beta_M \Delta e_T$$

$$\Delta e_\sigma = \Delta e_\rho + \alpha_M \Delta e_T$$

$$\Delta e_\pi = -\Delta e_\rho - \frac{n_x}{M} \Delta e_u + \alpha_M(\gamma-1)(1+n_x M)\Delta e_T$$

where Δe_τ, Δe_σ, and Δe_π are the vorticity, entropy, and sound sensitivity coefficients, respectively, and n_x is the direction cosine of the normal to the sound plane wave front relative to the flow direction. If the flow field is characterized by more than one sound direction, that is, if two or more significant sound sources with distinct orientations exist in the flow field, additional sound sensitivity coefficients would be required, one for each sound wave direction.

The hot-wire voltage fluctuation equation can now be rewritten as

$$\Delta e = \Delta e_\tau(\tau) + \Delta e_\sigma(\sigma) + \Delta e_\pi(\pi)$$

The mean-square voltage fluctuation output of the hot wire is given by

$$(\tilde{e})^2 = \Delta e_\tau^2(\tilde{\tau})^2 + \Delta e_\sigma^2(\tilde{\sigma})^2 + \Delta e_\pi^2(\tilde{\pi})^2 + 2\Delta e_\tau \Delta e_\sigma(\tilde{\tau})(\tilde{\sigma}) R_{\tau\sigma}$$
$$+ 2\Delta e_\sigma \Delta e_\pi(\tilde{\sigma})(\tilde{\pi}) R_{\sigma\pi} + 2\Delta e_\pi \Delta e_\tau(\tilde{\pi})(\tilde{\tau}) R_{\pi\tau}$$

where (~) again denotes the rms value of the fluctuation and each R is a correlation coefficient identified by its subscripts. In principle, six equations in six unknowns (the three fluctuations, $\tilde{\tau}$, $\tilde{\sigma}$, and $\tilde{\pi}$ and the three correlation coefficients) could be obtained for simultaneous solution if measurements were made at six distinct wire heating currents. (This would not be true if the orientation n_x of the sound wave were multivalued, since additional sensitivity coefficients and correlation coefficients would be introduced.) In reality, however, the determination of the sensitivity coefficients and the measurement of the rms voltage $\tilde{e}$ have uncertainties which rule out this method of solution (Ref. 10).

Depending on the nature of the flow in which the measurements are made, usually some of the terms in the equation for $(\tilde{e})^2$ can be neglected, being of the order of the uncertainties or small relative to the remaining terms. Specifically, the correlation coefficients ($R_{\pi\tau}$ and $R_{\sigma\pi}$) are almost always negligible because the nature of sound

propagation differs basically from the manner of vorticity and entropy propagation (Refs. 1 and 10). Moreover, Morkovin (Ref. 10) states that the three modes appear to be uncorrelated in the free stream of supersonic tunnels; that is,

$$R_{\tau\sigma} = R_{\sigma\pi} = R_{\pi\tau} = 0$$

The hot-wire equation then reduces to

$$(\tilde{e})^2 = \Delta e_\tau^2(\tilde{\tau})^2 + \Delta e_\sigma^2(\tilde{\sigma})^2 + \Delta e_\pi^2(\tilde{\pi})^2$$

or

$$Y^2 = (\tilde{\sigma})^2 + (\tilde{\tau})^2 X^2 + (\tilde{\pi})^2 (g_1 + g_2 X)^2$$

where

$$X = \frac{\Delta e_\tau}{\Delta e_\sigma} \text{ and } Y = \frac{\tilde{e}}{\Delta e_\sigma}$$

and

$$\frac{\Delta e_\pi}{\Delta e_\sigma} = g_1 + g_2 X$$

with

$$g_1 = \frac{-(\gamma-1)(M^2-1)}{1 + (\gamma-1)M^2}$$

$$g_2 = \frac{\gamma(1+n_x M)-(M^2-1)(n_x M)}{1 + (\gamma-1)M^2}$$

Hot-wire measurements provide the information needed to compute values for X and Y in plotting "direct" mode diagrams. If a value for n_X is assumed, the equation can be graphically solved for values of $\tilde{\tau}$, $\tilde{\sigma}$, and $\tilde{\pi}$, using methods given in detail by Morkovin (Ref. 10). The reliability of these procedures is improved by increasing the number of measurements, that is, the number of distinct wire heating currents for which data are obtained, to the extent that the additional points improve upon the accuracy of the fairing curves.

3.2 RESULTS

Measurements with a constant-current hot-wire anemometer were made in the free stream of the Tunnel D test section at Mach number 4 for three unit Reynolds numbers: 0.05, 0.12, and 0.24 million per inch. The measurements were made with the wire positioned on the tunnel centerline at the centerline of the test section windows, 55.1 in. from the nozzle throat, and parallel to the flexible plates of the nozzle. Information regarding the nature of the Tunnel D wall boundary layers has

been presented by Bell in Ref. 18. From Bell's measurements it was determined that the wall boundary layers at the window centerline were transitional for Re/in. = 0.05 million and were fully turbulent for Re/in. = 0.12 and 0.24 million.

The hot-wire measurements from the present investigation have been presented in various forms in Figs. 6 through 10. The data were obtained using the input transformer set on the higher frequency range (1 tc 320 kHz). (Signals recorded on the lower frequency range (25 Hz to 40 kHz) of the transformer were in general identical in rms voltage fluctuation level to those recorded on the higher range.) The low-frequency cut-off was set at 1 Hz and the high-frequency cut-off at 160 kHz. The time constant of the wire was determined by the square-wave technique for each measurement point. Each measurement was subsequently corrected for the electronic noise of the hot-wire instrumentation. The corrected data were reduced in accordance with the equations presented in the preceding section.

The data are presented in Fig. 6 in the form of the Kovasznay-type of mode diagram, that is, $\tilde{e}/\Delta e_T$ plotted versus $\Delta e_m/\Delta e_T$. For each unit Reynolds number, a straight line is the best simple fairing for the data, and this is in accord with the findings of Laufer (Ref. 4) for free-stream flow fluctuations in the working section of a supersonic wind tunnel. Data for wire overheat values ($a'_w = (R_w - R_r)/R_r \leq 0.56$) have been included in these diagrams. The measurements at higher overheat were not used because the temperature sensitivity Δe_T was a small positive number or a negative number, and, consequently, the coordinates were quite large (with an amplified uncertainty) or negative. This difficulty is mathematical in nature and pertains to the Kovasznay-type of mode diagram. Data at high overheat values may be handled by using the "direct" or Morkovin-type of mode diagram.

By following the arguments of Laufer (Ref. 4), the only simple fluctuating field which is consistent with the straight-line (positive slope) relation is a pure sound field in which the isentropic relation between the fluctuating quantities holds. Therefore,

$$\frac{\Delta p}{\bar{p}} = \gamma \frac{\Delta \rho}{\bar{\rho}} = \frac{\gamma}{\gamma - 1} \frac{\Delta T}{\bar{T}}$$

and

$$\frac{\Delta m}{\bar{m}} = \frac{\Delta u}{\bar{u}} + \frac{1}{\gamma} \frac{\Delta p}{\bar{p}}$$

$$\frac{\Delta T_o}{\bar{T}_o} = a_M(\gamma - 1)\left(\frac{\Delta p}{\gamma \bar{p}} + M^2 \frac{\Delta u}{\bar{u}}\right)$$

The basic equation can now be written

$$\frac{\Delta e}{\Delta e_T} = \alpha_M(\gamma-1)\left(\frac{\Delta p}{\gamma\bar{p}} + M^2\frac{\Delta u}{\bar{u}}\right) - \frac{\Delta e_m}{\Delta e_T}\left(\frac{\Delta p}{\gamma\bar{p}} + \frac{\Delta u}{\bar{u}}\right)$$

The mean-square voltage is now

$$\frac{\overline{(\Delta e)^2}}{\Delta e_T^2} = \left[\alpha_M(\gamma-1) - \frac{\Delta e_m}{\Delta e_T}\right]^2 \frac{\overline{(\Delta p)^2}}{\gamma^2\bar{p}^2} + \left[\beta_M - \frac{\Delta e_m}{\Delta e_T}\right]^2 \frac{\overline{\Delta u^2}}{\bar{u}^2} + 2\left[\alpha_M(\gamma-1) - \frac{\Delta e_m}{\Delta e_T}\right]\left[\beta_M - \frac{\Delta e_m}{\Delta e_T}\right] R_{up}\frac{\tilde{u}}{\bar{u}}\frac{\tilde{p}}{\gamma\bar{p}}$$

For the straight line relation in the flow diagram,

$$R_{up} = \frac{\overline{\Delta u\,\Delta p}}{\tilde{u}\tilde{p}} = -1$$

so that rms voltage can be expressed by

$$\frac{\tilde{e}}{\Delta e_T} = \left[\beta_M - \frac{\Delta e_m}{\Delta e_T}\right]\frac{\tilde{u}}{\bar{u}} - \left[\alpha_M(\gamma-1) - \frac{\Delta e_m}{\Delta e_T}\right]\frac{\tilde{p}}{\gamma\bar{p}} = \alpha_M(\gamma-1)\left(M^2\frac{\tilde{u}}{\bar{u}} - \frac{\tilde{p}}{\gamma\bar{p}}\right) + \left(\frac{\tilde{p}}{\gamma\bar{p}} - \frac{\tilde{u}}{\bar{u}}\right)\frac{\Delta e_m}{\Delta e_T}$$

By referring to Fig. 6, it is seen that the first term of the above equation is the ordinate intercept and the coefficient of $\Delta e_m/\Delta e_T$ is the slope of the data fairing. The fluctuations of density and velocity have been calculated from the intercept and slope information, and these, in turn, have been used to determine the magnitude of the other fluctuating quantities all of which are shown in Fig. 7[2], remembering that $R_{up} = -1.0$. It is seen that all of these fluctuation measurements increased with turbulent tunnel wall boundary layer thickness (decreasing unit Reynolds number).

The rms pressure fluctuations, normalized by the free-stream dynamic pressure ($\tilde{p}/q_\infty$), are shown in Fig. 8[2] plotted versus unit Reynolds number. Two data points obtained by Laufer (Ref. 4) from the 18- by 20-in. supersonic tunnel of the Jet Propulsion Laboratory at $M_\infty = 4$ are also shown. For both sets of data, the measured mean-square values have been divided by four, so that the data shown in Fig. 8 would correspond to radiations of the boundary layer of one tunnel wall. Laufer (Ref. 5) lists three assumptions which are required to justify this step: one, that the four tunnel wall boundary layers

---

[2]In Figs. 7, 8, and 9, an indication has been given of the possible effects on the fluctuation parameters of a change in the fairing of the mode diagrams. A possible data spread is shown which was determined by considering the maximum and minimum possible slopes of a linear fairing among the data for each unit Reynolds number (Fig. 6).

contribute equally to the sound measured at a given point in the free stream; two, that no correlations exist among the four radiated fields; and three, that no reflections occur from opposite walls. It is noted in Fig. 8 that the rms pressure fluctuations ($\tilde{p}/q_\infty$) measured for the smaller (12- by 12-in.) VKF Tunnel D are lower than those for the JPL (18- by 20-in.) tunnel. In either case, the fluctuation (sound) level increased with increased turbulent tunnel wall boundary layer thickness.

Laufer (Ref. 5) found that the Reynolds number effect on pressure fluctuations could be removed by normalizing by the average wall shearing stress. The measurements from the present investigation have been handled in this manner using values of shearing stress obtained from theoretical skin friction values determined by Van Driest's second method (Ref. 19) to normalize the pressure fluctuations, and, as can be seen in Fig. 9, the Reynolds number effect was almost entirely removed. Laufer's Mach number 4 results (from Fig. 12 of Ref. 4) have been treated in the same manner, and these results are also shown in Fig. 9.

By assuming that the fluctuation measurements have been made in the far-field of the sound source (that is, "many" wavelengths of the field away from the source), the sound waves may be considered to be plane (Ref. 4). The particle velocity fluctuation normal to the wave front ($|\Delta u_n|$) is related to the pressure variations by the equation

$$\frac{|\Delta u_n|}{\bar{u}} = \frac{1}{M}\frac{\Delta p}{\gamma \bar{p}}$$

Inasmuch as a hot wire is sensitive to velocity variations only in the direction of the mean flow, it follows that

$$\Delta u = |\Delta u_n| \cdot n_x$$

and

$$\frac{\Delta u}{\bar{u}} = \frac{1}{M}\frac{\Delta p}{\gamma \bar{p}} n_x$$

where n_x is the direction cosine of the normal to the wave front relative to the direction of the mean flow. The rms fluctuations can be related, with $R_{up} = -1$, by the equation,

$$\frac{\tilde{u}}{\bar{u}} = -\frac{1}{M}\frac{\tilde{p}}{\gamma \bar{p}} n_x$$

For the case of a stationary Mach wave, $n_x = -1/M$; then the rms pressure fluctuation associated with a fluctuating Mach wave is determined from the equation above to be

$$\frac{\tilde{p}}{\bar{p}} = \gamma M^2 \left(\frac{\tilde{u}}{\bar{u}}\right)$$

The equation for rms voltage with this substitution becomes

$$\frac{\tilde{e}}{Ae_T} = \left(1 - \frac{1}{M^2}\right)\left(\frac{\tilde{p}}{\gamma\bar{p}}\right)\frac{Ae_m}{Ae_T}$$

which is a straight line passing through the origin. Inasmuch as the straight lines of the mode diagrams of the present data do not pass through the origin (see Fig. 13 of Ref. 1), it is concluded that the related sound is not (primarily) radiated by unsteady Mach waves which originate from imperfections of the tunnel nozzle contour, joints, and similar generators, the so-called "shivering Mach waves" of Morkovin (Refs. 2 and 20). The possibility cannot be overlooked, however, that shivering Mach waves may co-exist with other sources of sound (see Section 4.1).

With the idea of a fixed disturbance as the primary source of the sound fluctuations ruled out, the concept of sound radiated by unsteady Mach waves, which originate from a moving source (Refs. 4 and 21), has been adopted.

With regard to Mach waves moving relative to the tunnel walls, if it is assumed that all sound fluctuations are generated from the same source, a preferred orientation can be derived. For this purpose, Laufer (Ref. 21) has adapted the theory of Phillips (Ref. 22) for the radiation of sound by a free shear layer to the case of boundary layer sound radiation. In essence, a frozen eddy pattern, like a wavy wall, moving downstream within the boundary layer, with a velocity relative to which the free-stream velocity is supersonic, radiates energy in the form of Mach waves. If the mean propagation velocity (streamwise) of the sound source is designated by $\bar{u}_s$, the mean velocity of the free stream relative to the virtual wavy wall is $\bar{u}_r = \bar{u} - \bar{u}_s$, and the corresponding Mach number is $M_r = \bar{u}_r/a = (\bar{u} - \bar{u}_s)/a = (-1/n_x) > 1$. Then, with $R_{up} = -1$,

$$\frac{\bar{u}_s}{\bar{u}} = 1 + \frac{1}{Mn_x} = 1 - \frac{\tilde{p}/\gamma\bar{p}}{M^2\,\tilde{u}/\bar{u}}$$

The propagation velocities calculated in this manner for the present hot-wire measurements are shown in Fig. 10, with two published values determined at $M_\infty = 4$ by Laufer (Ref. 4) for the 18- by 20-in. tunnel of the Jet Propulsion Laboratory. In comparison with the data from the JPL tunnel, the data from the VKF 12- by 12-in. tunnel exhibited a similar variation of sound-source propagation velocity with changing unit Reynolds number at $M_\infty = 4$, but the source velocity ratio was higher for the smaller tunnel for the range of unit Reynolds number investigated. The corresponding angle between the normal to the wave

front and the direction of the flow was between 122 and 128 deg for the three values of unit Reynolds number of the present data. If this orientation of the sound source is accepted for the present measurements, the hot wire on the tunnel centerline would not sense fluctuations radiated from the tunnel wall boundary layers which originated along the wall at less than 7 to 7.5 in. upstream of the window centerline.

It is seen from this discussion that the measurements of the present study are consistent with the assumption of a sound source moving streamwise within the tunnel wall boundary layer and radiating energy in the form of Mach waves.

With reference to the reasoning of Morkovin (Ref. 2) that vorticity and entropy fluctuations in the test section have their origin upstream of the nozzle (see Section I), the following additional information is supplied relative to Tunnel D: (1) An estimate was made for Tunnel D of the velocity fluctuations convected from the settling chamber into the test section at Mach number 4, based on the work of Ribner and Tucker (Ref. 23). The results indicate that rms velocity fluctuations are reduced to less than 0.004 percent of their magnitude in the settling chamber. (2) The temperature of the air supplied to Tunnel D is not directly controlled but is dependent on the temperature to which the air is heated in the high pressure air storage reservoir and on the pressure drop across the control valves which regulate stagnation pressure. Perforated baffle plates in the upstream diffuser between the valves and the settling chamber (Fig. 1c) cause the flow to mix, and the screens in the settling chamber further promote the decay of any temperature spots (entropy fluctuations) which are convected into the supply section. It is, therefore, concluded that vorticity and entropy fluctuations in the test section of Tunnel D are negligibly small and that the assumption of a pure sound field is well founded.

SECTION IV
DISCUSSION OF HOT-WIRE POWER SPECTRA

4.1 SPECTRAL ANALYSIS OF HOT WIRE DATA

Further sturcture information that characterizes the fluctuations in the flow field is obtained through the energy spectrum density of the hot-wire output. In this type of data analysis, the distribution of the kinetic energy of the fluctuations with frequency or wave number is given.

When seeking to separate the modes, an additional parameter, the frequency, must be added to the separating techniques of the preceding section. For example, the mean-square voltage fluctuation output of the hot wire becomes at each frequency (Ref. 10):

$$E_e(f,A'_w) = \Delta e_r^2(A'_w)F_r(f) + \Delta e_\sigma^2(A'_w)F_\sigma(f) + \Delta e_\pi^2(A'_w,f)F_\pi(f) + 2\Delta e_r\Delta e_\sigma\sqrt{F_r(f)F_\sigma(f)}\,R_{r\sigma}(f)$$
$$+ 2\Delta e_\sigma\,\Delta e_\pi\sqrt{F_\sigma(f)F_\pi(f)}\,R_{\sigma\pi}(f) + 2\Delta e_\pi\,\Delta e_r\sqrt{F_\pi(f)F_r(f)}$$

where

$$(\overline{e})^2 = \int_0^\infty E_e(f)df \text{ and } (\overline{i})^2 = \int_0^\infty F_i(f)df \text{ for } i = r,\sigma,\pi$$

where the symbol F refers to rms quantities at the frequency f, each R is a correlation coefficient identified by its subscripts, and the parentheses denote functional relationships. As before, this equation is based on an assumption of a single dominant sound source. In the presence of all three modes and their correlations, the calibration would require at least six different overheats at as many frequencies as possible. For the case of the present measurements, the data indicate the dominance of the sound mode, as discussed in the preceding sections, and the equation reduces to

$$E_e(f,A'_w) = \Delta e_\pi^2(A'_w,f)F_\pi(f)$$

for a single sound source.

Ideally, the energy spectral density is obtained as

$$\Delta e_\pi^2(A'_w,f)F_\pi(f) = \lim_{\Delta f \to 0}\ \lim_{t \to \infty}\ \frac{1}{\Delta f}\int_0^t E_e(f,A'_w)dt$$

where $E_e(f, A'_w)$ is the square of the signal time function in an infinitely narrow band (Δf) averaged over an inifinitely long time (t). Under the assumption that the fluctuation signal is stationary and ergodic, a system of narrow-band filters using a finite time (t) and a finite bandwidth (Δf) can be used to obtain the spectrum. In so doing, a relative statistical error is introduced which for an ideal filter is (Ref. 24):

$$\text{error} = \frac{s}{E(f,A'_w)} = \frac{1}{\sqrt{\Delta ft}}$$

where s is the standard deviation and $E(f, A'_w)$ is the experimentally determined spectrum. For the case of the measurements reported herein, $\Delta f = 50$ Hz and $t = 4$ sec, yielding a statistical uncertainty of $\sim\pm 7.0$ percent.

Further complicating the experimental determination of the energy density function is the matching of the anemometer compensation amplifier to the wire frequency roll-off so that the wire has an effective flat frequency response. This is accomplished through the time constant setting in the amplifier. If the time constant is properly set, the frequency response is as indicated in Fig. 11a. However, as was mentioned in the preceding section, because of experimental difficulties, a degree of uncertainty in the selection of the time constant was inherent in the experiment. The effect of improper compensation on the wire response is shown in Figs. 11b and c. As a result of this effect some distortion of the measured spectra can be anticipated.

In interpreting the measured spectra when the fluctuations are considered to be sound-induced, the relative propagation of the sound mode introduces a frequency distortion when sensed by a stationary hot wire. This is illustrated by considering a plane wave with the wave vector inclined to the mean flow direction by an angle θ. The frequency is given by $f = \frac{a + \bar{u} \cos \theta}{\lambda} = \frac{a}{\lambda}(1 + M \cos \theta)$, and when $\cos \theta = -1/M$, a Mach wave, the frequency indicated by the wire is zero. Consequently, it can be inferred that frequencies near zero represent Morkovin's "shivering Mach waves" (Refs. 2 and 20). For this special case, the corresponding mode diagrams would pass through the origin, as was pointed out in the previous section, and the equation for the sensitivity coefficient Δe_π (see Section 3.1) would use the substitution $n_x = -1/M$. However, a non-zero value of the intercept indicates a traveling sound source with a dominant orientation other than that of a Mach wave. In this case, the applicable direction cosine is that calculated from the average source velocity. For computational purposes, the model allows only one sound source (otherwise a second sound sensitivity coefficient must be included). It must be pointed out again that this does not rule out the possibility that the real physical situation may include both "shivering Mach waves" and a traveling sound source.

A further complicating factor in interpreting the spectra occurs because of the directional sensitivity of the wire through the overheating parameter (A'_w). Inspection of the sound sensitivity coefficient Δe_π reveals (Ref. 11) that a value of A'_w can be found for which Δe_π (Table I) is independent of sound direction. In reporting the results herein, the data have been grouped according to the alternate overheat (a'_w) and reported for the various unit Reynolds numbers.

A more nearly precise comparison of spectra could have been made with a constant sensitivity coefficient ratio ($\Delta e_m / \Delta e_T$). With this coefficient ratio maintained constant, the sensitivity of Δe_π to the sound

wave direction would be constant. This technique was not utilized in the present study because the required calculations are quite lengthy and the computer program was being developed simultaneously with the acquisition of data.

An exemplary variation of $\Delta e_m/\Delta e_T$ with certain nominal values of overheat and with unit Reynolds number is shown below:

Nominal Overheat, a_w =	0.05	0.4	0.5
Re/in. $= 0.05 \times 10^6$	0.134	1.57	2.47
$= 0.12 \times 10^6$	0.126	1.37	2.71
$= 0.24 \times 10^6$	0.104	1.50	2.76

The free-stream measurements indicate a useful energy content in the signal to a frequency of about 80 kHz. At this point, the signal approached the noise level of the hot-wire instrumentation as shown in Fig. 12. Moreover, if the upper frequency limit of the hot-wire system is defined as the frequency at which the signal is attentuated to 0.707 (3 db) of its amplitude at zero frequency, the "ceiling-to-floor" ratio (= 500) of the amplifier imposes a lower bound for the various upper frequency limits of this study (wherein the time constants had an upper limit of ~1.0 msec) of ~80 kHz. This limitation, it must be pointed out, is not an explanation of the roll-off of the hot-wire signal in Fig. 12; the system limitation is based on the 3-db point, whereas the hot-wire signal at 80 kHz was down by 24 db from its level at f = 10 kHz.

Inspection of the analysis plots indicated that the most significant signal fluctuation frequencies were below 20 kHz, while above this frequency all spectra appear to decay in an orderly manner; for this reason, only the portion of the spectra below 20 kHz is considered in the succeeding discussion.

The method of spectral data presentation selected for Fig. 13 is that suggested by Liepmann, Laufer, and Liepmann (Ref. 25) in which

$$\left[\widetilde{\pi(f)}\right]^2 df = [\widetilde{\pi}]^2 G(f) df$$

where

$\left[\widetilde{\pi(f)}\right]^2$ is the sound energy density at f

$[\widetilde{\pi}]^2$ is the total sound energy

and $G(f)$ is the normalized sound energy density distribution function satisfying the condition $\int_0^\infty G(f)df = 1$

The particular advantage of this form lies in the elimination of the calibration coefficients, since

$$\frac{\left[\widetilde{\pi(f)}\right]^2}{[\tilde{\pi}]^2} = \frac{E_e(f)}{(\tilde{e})^2} = G(f)$$

The normalized sound energy density is obtained from the energy density distribution by

$$\left[\widetilde{\pi(f)}\right]^2 = [\tilde{\pi}]^2 G(f)$$

where $\tilde{\pi}$ is obtained as indicated in Section 3.1. This particular data presentation technique is less clear whenever there is an uncertainty of the direction cosine n_x of the sound wave.

As a final note of caution in interpreting the data, the above techniques have specifically ruled out the existence of other modes; that is, entropy, vorticity, or another sound source. The conclusion that they contribute only negligibly to the turbulence energy is reasonably justified, but on the other hand, they may contribute significantly as an effect on other phenomena.

4.2 RESULTS

Power spectral density analyses of the hot-wire signal were obtained for three nominal wire overheats, $a_w' = 0.05$, 0.4, and 0.5, at each of the three unit Reynolds numbers of the present study, and the results are presented in various forms in Figs. 13 through 15. An uncertainty of ±1 db is estimated for the power spectral density traces (which are not shown), and the corresponding uncertainty interval is indicated in each figure for several signal frequencies for the data obtained at Re/in. $= 0.12 \times 10^6$; these intervals are typical of all three values of Re/in.

The normalized energy density distribution for the nominal overheats is presented in Fig. 13 for frequencies $f \leq 20$ kHz. The lack of similarity of the spectra for a given unit Reynolds number and different overheats is a result of the dependence of the sound sensitivity on overheat (Ref. 16). The differences in shape at each overheat warrant discussion of each set separately. The low overheat ($a_w = 0.05$) data plot (Fig. 13a) exhibits sharp peaks at frequencies less than 1 kHz. The maximum peak is at the lowest unit Reynolds number, the lowest peak

is at the intermediate unit Reynolds number, and the highest unit Reynolds number has the intermediate peak, thus indicating the following trend: as the unit Reynolds number increased, the amplitude of the low frequency portion of the spectrum ($f < 1$ kHz) at first decreased and then increased. A similar trend is exhibited at the higher overheat, $a'_w = 0.4$, where the signal amplitude is much larger. Inspection of the plots for all three overheats in Fig. 13 reveals that the amplitude at any given frequency $f \geq 1$ kHz was essentially the same, within experimental error, for both the intermediate and highest unit Reynolds numbers. When the normalized sound energy density[3] is plotted, as in Fig. 14, it is seen that in general the normalized sound energy density $\left[\overline{\pi(f)}\right]^2$ decreased with increasing unit Reynolds number in the low frequency range. It should be mentioned that this low frequency effect is much more pronounced than is indicated by the mean square fluctuation quantities. If the data for Re/in. $= 0.05 \times 10^6$ are taken as a reference, the percentage change of the peak values for the remaining unit Reynolds numbers varies from 60 to 89 percent for the three overheats. This is in contrast to a maximum change of 50 percent in the mean square fluctuation, $(\overline{\pi})^2$.

Laufer (Ref. 5) and Laufer, Ffowcs Williams, and Childress (Ref. 26) have found that the use of an integral scale to normalize "far field" energy density spectra at Mach numbers 2.0 and 4.5 produced very similar distributions for the two Mach numbers. It can be concluded that in addition to the mean-square fluctuation which characterizes the flow, an additional parameter, such as a length scale, is needed to characterize the spectral shape. In lieu of the integral scale as developed in Ref. 5, the thickness (δ) of the tunnel wall boundary layer was chosen for normalizing the present data for a similar presentation (Fig. 15). The values used for δ were taken from the measurements made by Bell (Ref. 18) at the window centerline station of Tunnel D.

The normalized energy spectra for the three Reynolds numbers of the present study at an overheat of $a'_w = 0.4$ have been presented in Fig. 15 in the form $u_\infty G(f)/\delta$ plotted against $f\delta/u_\infty$, for frequencies 250 Hz $\leq f \leq$ 80 kHz. Data for the two higher values of unit Reynolds number are in excellent agreement for $f\delta/u_\infty > 0.035$ (that is for $f > 700$ Hz). Moreover, at lower frequencies where the time constant of the analysis equipment is relatively long, the uncertainty of the results is probably greater than indicated; in which event, the separation

[3]It has been assumed that the spectra are sound dominated and result from a single source with an average direction cosine determined from the mode diagram analysis.

of the two curves may lack significance. With a decrease in unit Reynolds number to 0.05×10^6 per inch, more energy becomes concentrated at the lower frequencies, while for intermediate frequencies ($3\,kHz \leq f \leq 20\,kHz$) the differences among the three curves was not significant. For higher frequencies ($f > 20\,kHz$), the level of the hot-wire signal for the lowest unit Reynolds number (0.05×10^6 per inch) approached the level of the electronic noise of the hot-wire equipment (within 3 db) and, therefore, was considered to be no longer meaningful in this frequency range.

The explanation offered by Laufer, Ffowcs Williams, and Childress (Ref. 26) for the behavior of pressure spectra in the far field was obtained through the "eddy Mach wave" concept. In this model, the eddy scales in the turbulent boundary layer determine the scales (wavelengths) of the radiated sound. For an increasing unit Reynolds number, the wall boundary layer thickness decreases with the result that the energy-containing eddies become smaller, and this forces a shift of the energy density spectra to higher frequencies. Further investigation should be made of the power spectra of the radiated sound mode so that the disturbances can be more nearly completely characterized.

SECTION V
DISCUSSION OF SURFACE PRESSURE FLUCTUATIONS ON A FLAT PLATE

In order to relate the tunnel wall radiated sound measured in the free stream by the hot-wire technique to pressure fluctuations measured on a model surface, a flat plate instrumented with a flush-mounted microphone was installed in the test section of Tunnel D at the conclusion of the hot-wire measurements. The 8-in.-long, 5-in.-wide flat plate (Fig. 3) used by Pate and Schueler (Ref. 6) was mounted with the flat surface located 1.2 in. above the tunnel centerline (for $\phi = 0$) and with the microphone positioned axially at the window centerline.

Data were obtained at the following nominal tunnel conditions:

p_o, psia	Re/in. $\times 10^{-6}$
3	0.025
6	0.050
15	0.12
30	0.24
60	0.48

The results normalized by the free-stream dynamic pressure are presented in Fig. 16. Similar measurements obtained with the flat plate rotated counterclockwise about the tunnel centerline (ϕ = -90 deg) have been included also. The hot-wire anemometry results from the present study, apportioned for the radiation of a single tunnel wall (Fig. 3), are shown again in Fig. 16, for comparison purposes. Regarding the microphone data, it is noted that the measurements at Re/in. = 0.12×10^6, 0.24×10^6, and 0.48×10^6 are effectively equal. For Re/in. = 0.05×10^6, the pressure fluctuations were generally lower; whereas at Re/in. = 0.025×10^6, the measurements were an order of magnitude lower. The data obtained with the microphone oriented toward the tunnel sidewall (ϕ = -90 deg) were in general somewhat lower than those recorded with the microphone oriented toward the flexible plate (ϕ = 0), but, by noting the spread in the measurements for ϕ = 0, these differences may lack significance. In the calculations, no attempt was made to correct the data for the attenuation of microphone response which would be expected because of the finite size of the microphone diaphragm (0.25-in.-diam) compared with the short wave lengths contained among the fluctuations (Refs. 27 and 28).

The magnitude of free-stream pressure fluctuations at Re/in. = 0.025×10^6 would be of interest for a comparison with the microphone data; unfortunately, the hot-wire measurements were not extended below a value of Re/in. of 0.05 million. However, Vrebalovich has reported (Ref. 29) that free-stream fluctuation levels were found to be smaller when the tunnel wall boundary layer was laminar than when it was turbulent. Therefore, with decreasing unit Reynolds number, a fall-off in free-stream pressure fluctuation level somewhere below the value for Re/in. of 0.05 million would be expected from hot-wire measurements in Tunnel D.

The Tunnel D wall boundary layer thickness measurements by Bell (Ref. 18) indicate that the flexible plate boundary layer was transitional at the window centerline station for values of unit Reynolds number between 0.04 and 0.08 million per in. (By using the orientation of the sound source derived in Section 3.2 and noting again that the flat-plate surface was located 1.2 in. off tunnel centerline, it follows that the microphone would not receive sound radiation which originated along the tunnel wall at less than 5.5 to 6 in. upstream of the window centerline.) It is, therefore, concluded that the present microphone data for Re/in. = 0.025 and 0.05 million were associated with sound radiated by laminar and transitional tunnel wall boundary layers, respectively.

Moreover, if one considers the findings of Pate and Brown (Ref. 31) and Pate and Schueler (Figs. 5 and 6 of Ref. 6), it could be inferred that the maximum sound radiation would be associated with the completion of transition; in which event, the free-stream fluctuations probably attained a higher level than any actually measured in the present investigation, that is, between present values of unit Reynolds number. This reasoning led to the fairing included in Fig. 16, although the level and precise unit Reynolds number of the maximum are necessarily arbitrary, here.

A comparison of the two sets of measurements shown in Fig. 16 reveals that the pressure fluctuations determined by the microphone under the boundary layer of the flat plate were 20 to 45 times larger than those determined in the free stream by the hot wire. This magnitude of amplification of pressure fluctuations by the flat plate boundary layer is consistent with the recent findings of Kendall (Ref. 31) at a Mach number of 4.5 in the JPL 18- by 20-in. tunnel. The implication is that the laminar boundary layer over its 3.5-in. length is responsible for at least a 20-fold amplification or accumulation of free-stream pressure fluctuations. It should be noted again that the microphone measurements have been presented without any corrections for attenuation of response resulting from the finite size of the sensor and are, therefore, conservative.

A power spectral density analysis of the microphone output recorded at Re/in. = 0.24×10^6 is presented in Fig. 17 which is representative, except for signal level, of all analyses of microphone signals recorded in the present investigation. The output signal was analyzed using a bandwidth of 50 Hz for the frequency range shown in the figure. The trace is characterized by several outstanding peaks which, in general, were found in all of the analyses. The most prominent of the peaks, at f = 45 kHz, is the result of the microphone resonance previously discussed. The sources of the remaining peaks are unknown, but signals from the hot wire in the free stream for the same tunnel condition do not exhibit these spikes. Whether they are related to the microphone, to the amplification by the flatplate boundary layer, or to some other cause should be investigated.

The power spectra for a set of microphone data points which spanned the range of unit Reynolds numbers from Re/in. = 0.025×10^6 to 0.48×10^6 are compared in Fig. 18. The similarity of the shapes of the microphone energy density spectra, especially for Re/in. $\geq 0.05 \times 10^6$,

was not expected. This peculiarity also should be investigated to determine if it is an actual physical phenomenon or was a measurement idiosyncrasy. This presentation shows that, with increasing unit Reynolds number, the level of the signal at each frequency rose to an essentially constant value associated with the tunnel conditions (Re/in. = 0.12×10^6 and 0.24×10^6) for which the tunnel wall boundary layers were turbulent. The trace presented for Re/in. = 0.48×10^6, however, reveals a trend not obvious among the rms pressure fluctuation data (Fig. 16), namely another rise in signal level with the tunnel wall boundary layer already fully turbulent. An examination of Schlieren photographs made of the flow over the flat plate as the microphone data were being recorded revealed that the flat-plate boundary layer was laminar at the microphone station for Re/in. $\leq 0.24 \times 10^6$ and had become transitional for Re/in. = 0.48×10^6. It is concluded from this evidence that the increase in the level of the power spectra shown for the latter unit Reynolds number was a result of the change in the nature of the flat-plate boundary layer above the microphone.

The lack of an analytic theory and the widely different measurement characteristics of the hot wire and the microphone leave the nature of the interactions of free-stream and flat-plate boundary layer fluctuations unresolved in this investigation. An interesting extension of this study could be performed with a hot wire immersed in a flat-plate boundary layer that has a flush-mounted microphone so that both sensors experience the same flow field.

SECTION VI
CONCLUDING REMARKS

Hot-wire anemometry techniques were successfully employed to determine free-stream flow fluctuations at a Mach number of $M_\infty = 4$ in the test section of the 12- by 12-in. supersonic tunnel (D). The results are quite similar to findings at $M_\infty = 4$ in another tunnel which have been published by Laufer. It was found that each of the various fluctuations deduced from the hot-wire measurements increased with the thickness of the turbulent tunnel wall boundary layers. The Reynolds number effect on the pressure fluctuations was removed by normalizing by the average wall shearing stress. The free-stream measurements of the present study have been examined using the assumption of a sound source traveling in the tunnel wall boundary layer at a velocity relative to which the free-stream velocity is supersonic. The data exhibited an increase of the propagation velocity of the sound source with increasing unit Reynolds number.

Power spectral density analyses of the hot-wire output indicate that, in addition to the mean-square fluctuation characterizing the flow, an additional parameter such as a length scale is useful to characterize the spectral shape.

Supplementary measurements in the test section, for the same testing conditions as for the hot wire, using a microphone mounted flush with the surface of a flat plate, revealed pressure fluctuation levels larger than those of the free stream by a factor of at least 20. Further inquiry into the nature of the interactions between the free-stream fluctuations and the flat-plate boundary layer is needed to explain this phenomenon.

REFERENCES

1. Kovasznay, Leslie S. G. "Turbulence in Supersonic Flow." Journal of the Aeronautical Sciences, Vol. 20, No. 10, October 1953, pp. 657-674, 682.

2. Morkovin, M. V. "On Supersonic Wind Tunnels with Low Free-Stream Disturbances." Transactions of the ASME, Vol. 81, Series E - Journal of Applied Mechanics, Vol. 26, September 1959, pp. 319-324.

3. Laufer, John. "Factors Affecting Transition Reynolds Numbers on Models in Supersonic Wind Tunnels." Journal of the Aeronautical Sciences, Vol. 21, No. 7, July 1954, pp. 497, 498.

4. Laufer, John. "Aerodynamic Noise in Supersonic Wind Tunnels." Journal of the Aerospace Sciences, Vol. 28, No. 9, September 1961, pp. 685-692.

5. Laufer, John. "Some Statistical Properties of the Pressure Field Radiated by a Turbulent Boundary Layer." The Physics of Fluids, Vol. 7, No. 8, August 1964, pp. 1191-1197.

6. Pate, S. R. and Schueler, C. J. "Effects of Radiated Aerodynamic Noise on Model Boundary-Layer Transition in Supersonic and Hypersonic Wind Tunnels." AEDC-TR-67-236 (AD666644), March 1968.

7. Anderson, A. "Flow Characteristics of a 12-in. Intermittent Supersonic Tunnel." AEDC-TDR-63-203 (AD418578), September 1963.

8. Laufer, John and Vrebalovich, Thomas. "Stability and Transition of a Supersonic Laminar Boundary Layer on an Insulated Flat Plate." Journal of Fluid Mechanics, Vol. 9, Part 2, 1960, pp. 257-299.

9. Vrebalovich, Thomas. "Application of Hot-Wire Techniques in Unsteady Compressible Flows." Jet Propulsion Laboratory Technical Report No. 32-229, May 1962.

10. Morkovin, Mark V. "Fluctuations and Hot-Wire Anemometry in Compressible Flows." AGARDograph 24, November 1956.

11. Chu, Boa-Teh, and Kovasznay, Leslie S. G. "Non-Linear Interactions in a Viscous Heat Conducting Compressible Gas." Journal of Fluid Mechanics, Vol. 3, Part 4, 1958, pp. 494-514.

12. Laufer, John and McClellan, Robert. "Measurements of Heat Transfer from Fine Wires in Supersonic Flows." Jet Propulsion Laboratory Report No. 20-101, June 1957.

13. Dewey, C. Forbes, Jr. "A Correlation of Convective Heat Transfer and Recovery Temperature Data for Cylinders in Compressible Flow." International Journal of Heat and Mass Transfer, Vol. 8, 1965, pp. 245-252.

14. Kovasznay, Leslie S. G. "Turbulence Measurements." Section F, pp. 213-285 of Vol. 9, High-Speed Aerodynamics and Jet Propulsion, Princeton University Press, 1954.

15. Morkovin, Mark V. and Phinney, Ralph E. "Extended Applications of Hot-Wire Anemometry to High-Speed Turbulent Boundary Layers." AFOSR TN-58-469 (AD158279), June 1958.

16. Morkovin, Mark V. "Signal Interpretation in High-Speed Anemometry-A Review." in Advances in Hot-Wire Anemometry. edited by Melnik, W. L., and Weske, J. R., AFOSR Report No. 68-1492 (AD676019), July 1968, pp. 38-51.

17. Kovasznay, Leslie S. G. and Tornmarck, Sven I. A. "Heat Loss of Hot Wires in Supersonic Flow." Bumblebee Report No. 127 (ATI 84111), The Johns Hopkins University, April 1950.

18. Bell, D. R. "Boundary Layer Characteristics at Mach Numbers 2 through 5 in the Test Section of the 12-Inch Supersonic Tunnel (D)." AEDC-TDR-63-192 (AD418711), September 1963.

19. Van Driest, E. R. "The Problem of Aerodynamic Heating." Aeronautical Engineering Review, Vol. 15, No. 10, October 1956, pp. 26-41.

20. Morkovin, Mark V. "On Transition Experiments at Moderate Supersonic Speeds." Journal of the Aeronautical Sciences, Vol. 24, No. 7, July 1957, pp. 480-486.

21. Laufer, John. "Sound Radiation from a Turbulent Boundary Layer." Jet Propulsion Laboratory Technical Report No. 32-119, November 1961.

22. Phillips, O. M. "On the Generation of Sound by Supersonic Turbulent Shear Layers." Journal of Fluid Mechanics, Vol. 9, Part 1, 1960, pp. 1-28.

23. Ribner, H. S. and Tucker, M. "Spectrum of Turbulence in a Contracting Stream." NACA Report TR 1113, 1953.

24. Bendat, Julius S. and Piersol, Allc. ... Measurement and Analysis of Random Data. John Wiley and Sons, Inc., New York, 1966, p. 260.

25. Liepmann, H. W., Laufer, J., and Liepmann, Kate. "On the Spectrum of Isotropic Turbulence." NACA TN 2473, November 1951.

26. Laufer, John, Ffowcs Williams, John E., and Childress, Stephen. "Mechanism of Noise Generation in the Turbulent Boundary Layer." AGARDograph 90, November 1964.

27. Corcos, G. M. "Resolution of Pressure in Turbulence." The Journal of the Acoustical Society of America, Vol. 35, No. 2, February 1963, pp. 192-199.

28. Kistler, A. L. and Chen, W. S. "The Fluctuating Pressure Field in a Supersonic Turbulent Boundary Layer." Journal of Fluid Mechanics, Vol. 16, Part 1, May 1963, pp. 41-64.

29. Vrebalovich, Thomas. Discussion: "On Supersonic Wind Tunnels with Low Free-Stream Disturbances." by M. V. Morkovin, Journal of Applied Mechanics, June 1960, pp. 362, 363.

30. Pate, S. R. and Brown, M. D. "Acoustic Measurements in Supersonic Transitional Boundary Layers." Paper Presented at the 15th National Instrument Society of America (ISA) Aerospace Instrumentation Symposium at Las Vegas, Nevada, May 5-7, 1969. and AEDC-TR-69-182 (AD694071), October 1969.

31. Kendall, J. M., Jr. "Supersonic Boundary Layer Transition Studies." Section V-C of "Space Programs Summary 37-62 Vol. III: Supporting Research and Advanced Development." Jet Propulsion Laboratory, April 30, 1970, pp. 43-47.

Preceding page blank

APPENDIXES

I. ILLUSTRATIONS
II. TABLE

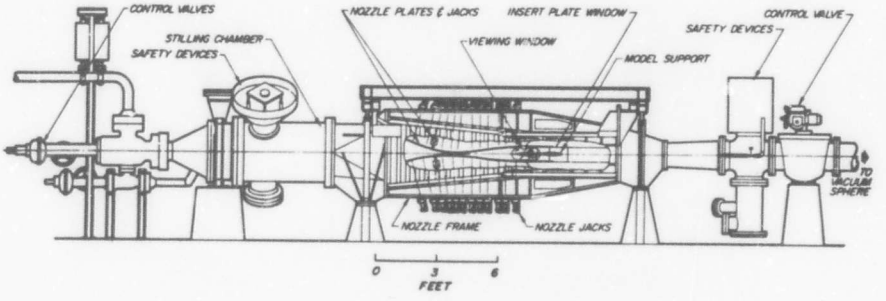

a. Assembly

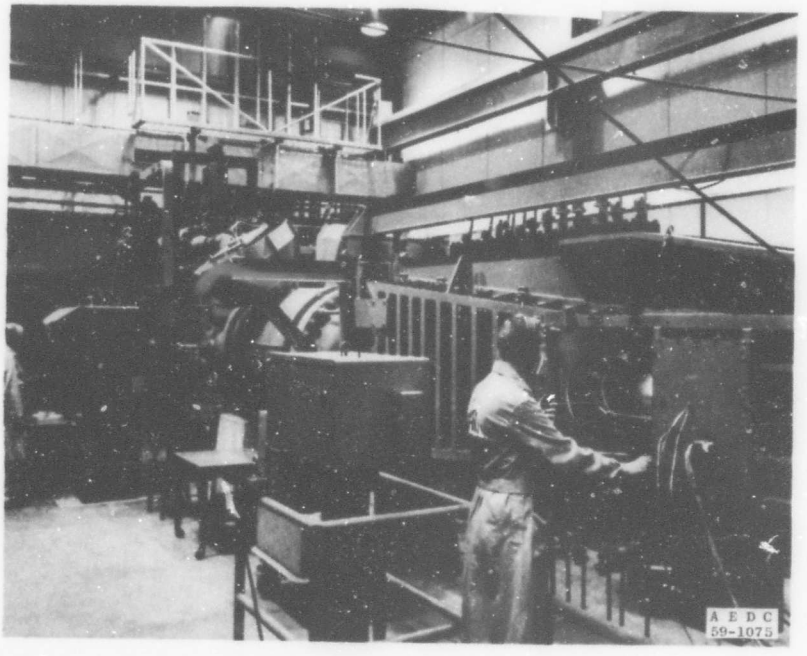

b. Photograph

Fig. 1 Tunnel D, a 12- x 12-in. Supersonic Wind Tunnel

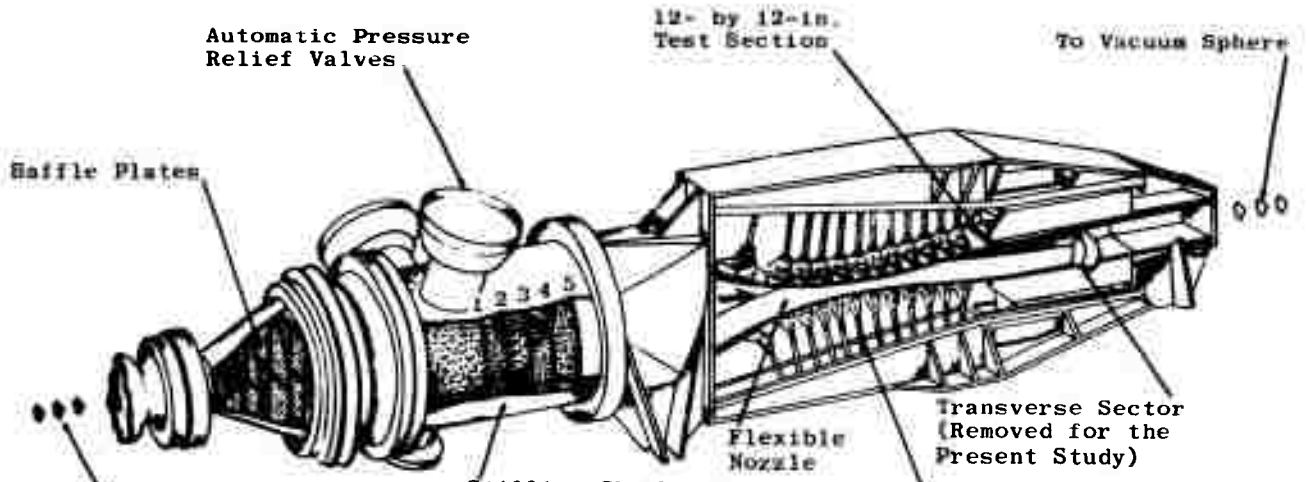

Screens	Mesh	Wire Diameter, in.
1-4	20	0.017
5	30	0.0065

c. Perspective Drawing

Fig. 1 Concluded

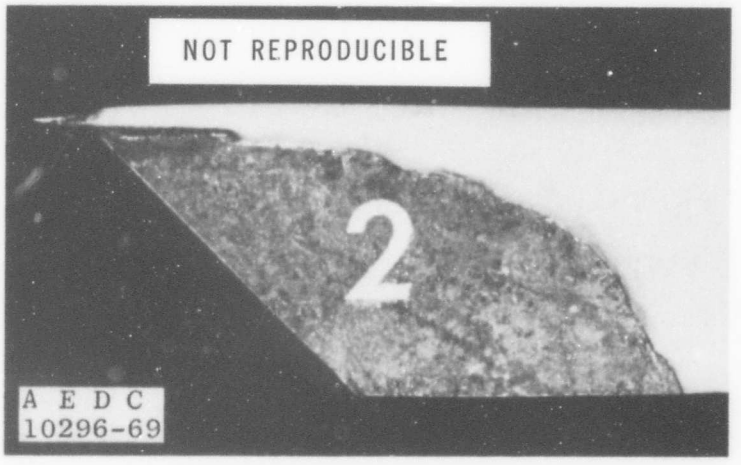

a. Side View

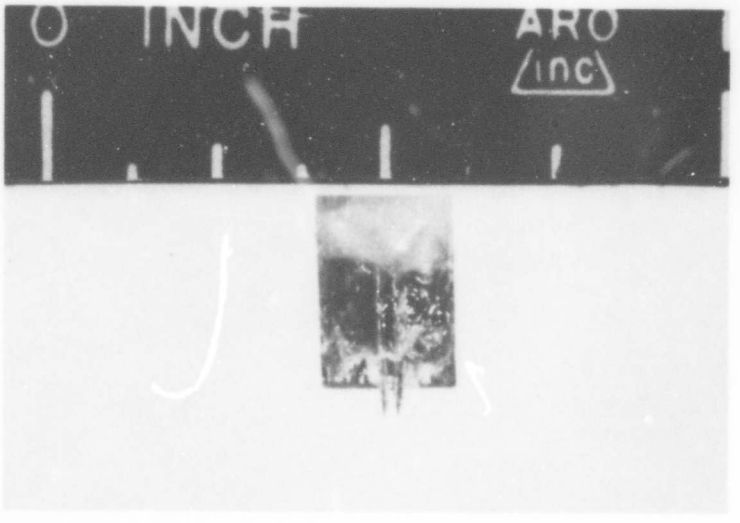

b. Top View
Fig. 2 Hot-Wire Probe

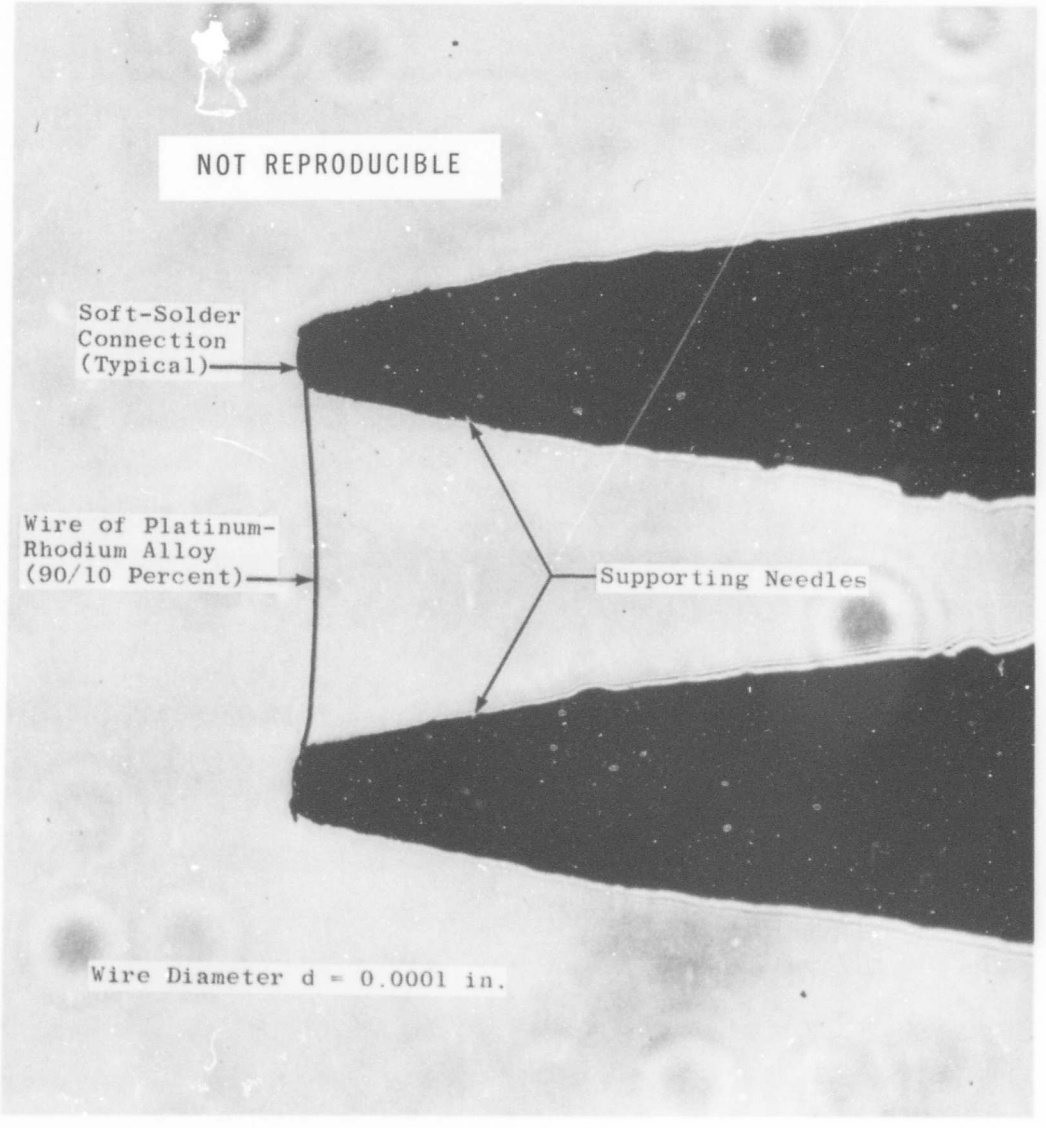

c. Shadowgram of a Typical Wire Attachment
Fig. 2 Concluded

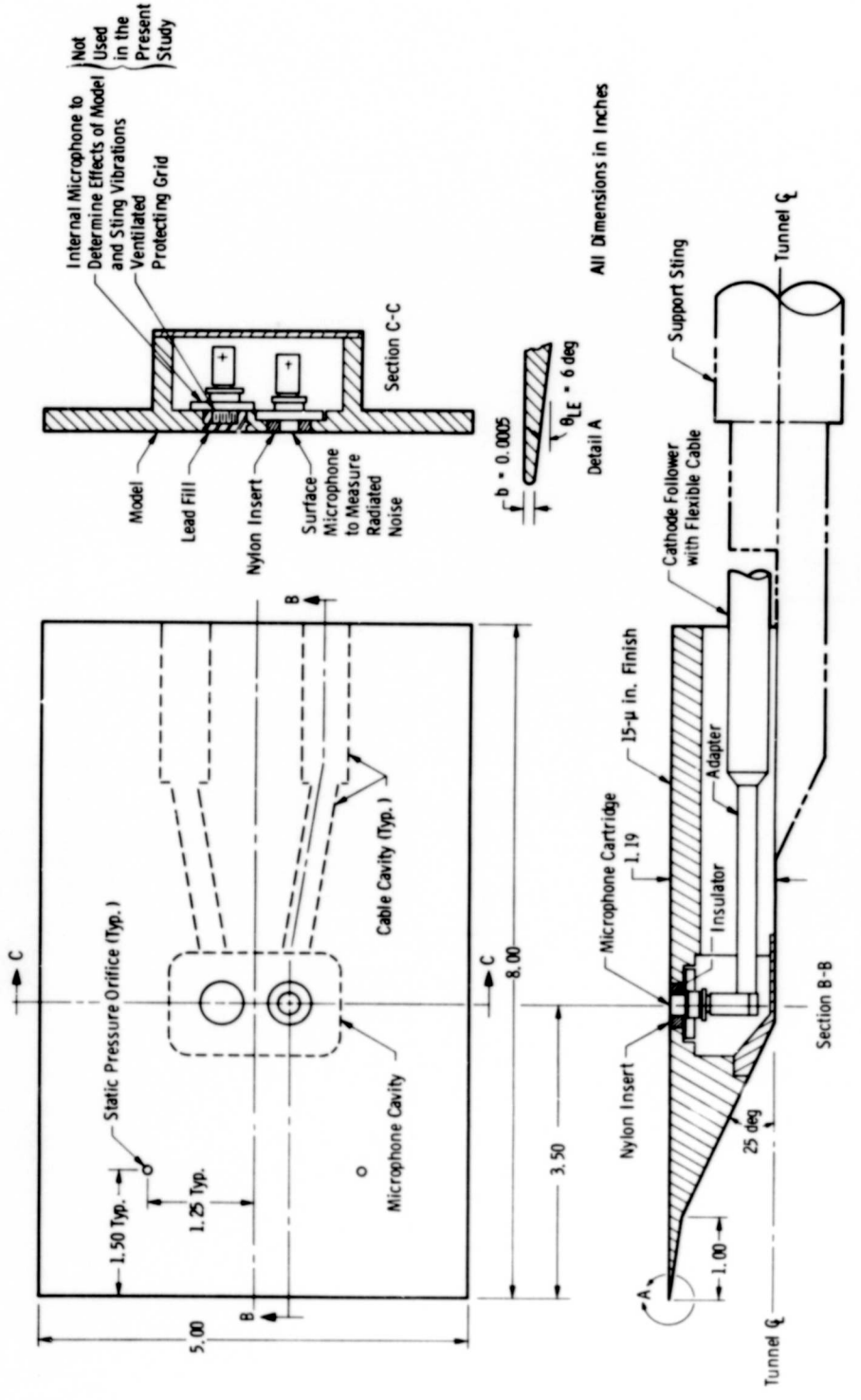

Fig. 3 Flat Plate Microphone Model

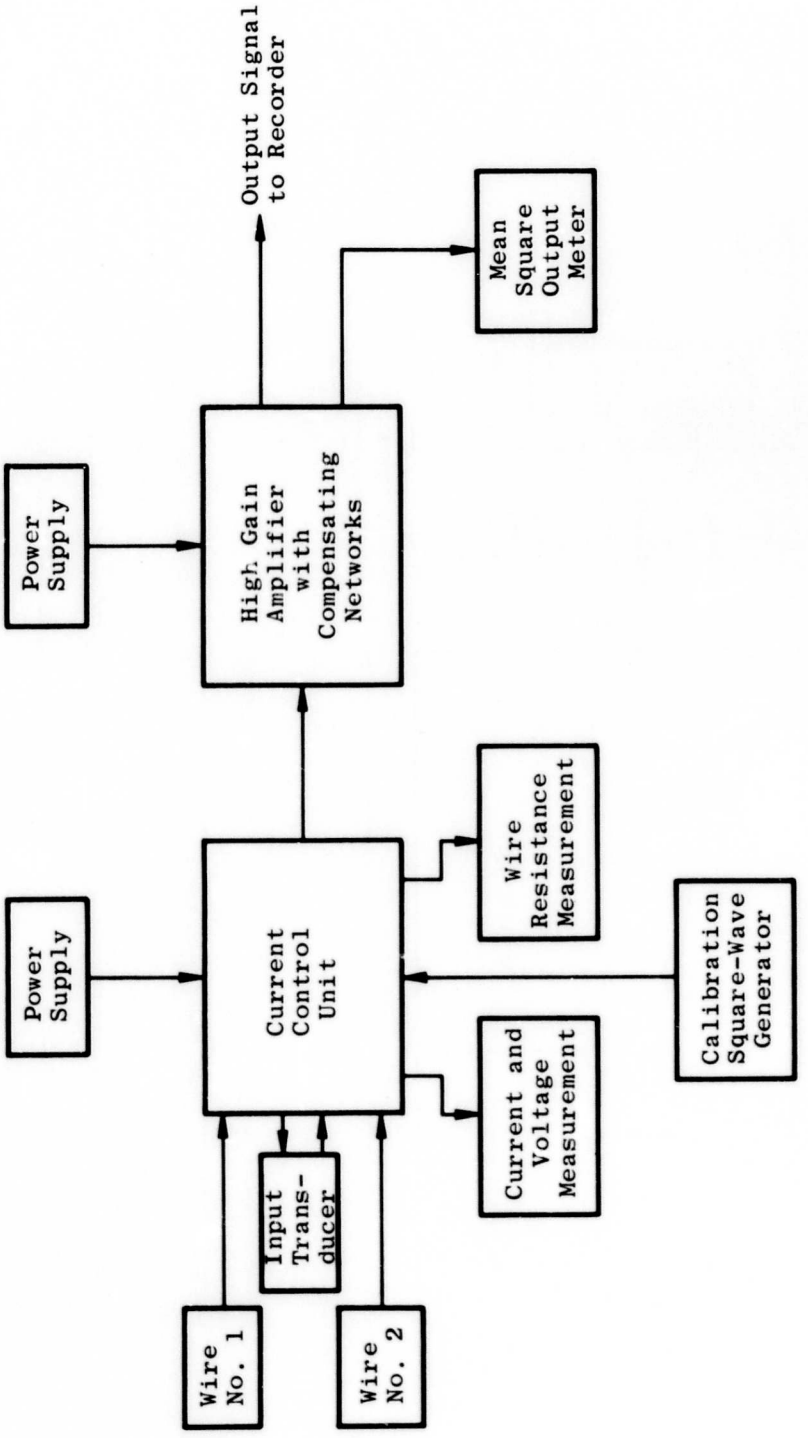

Fig. 4 Functional Block Diagram of Constant Current Hot-Wire Anemometer

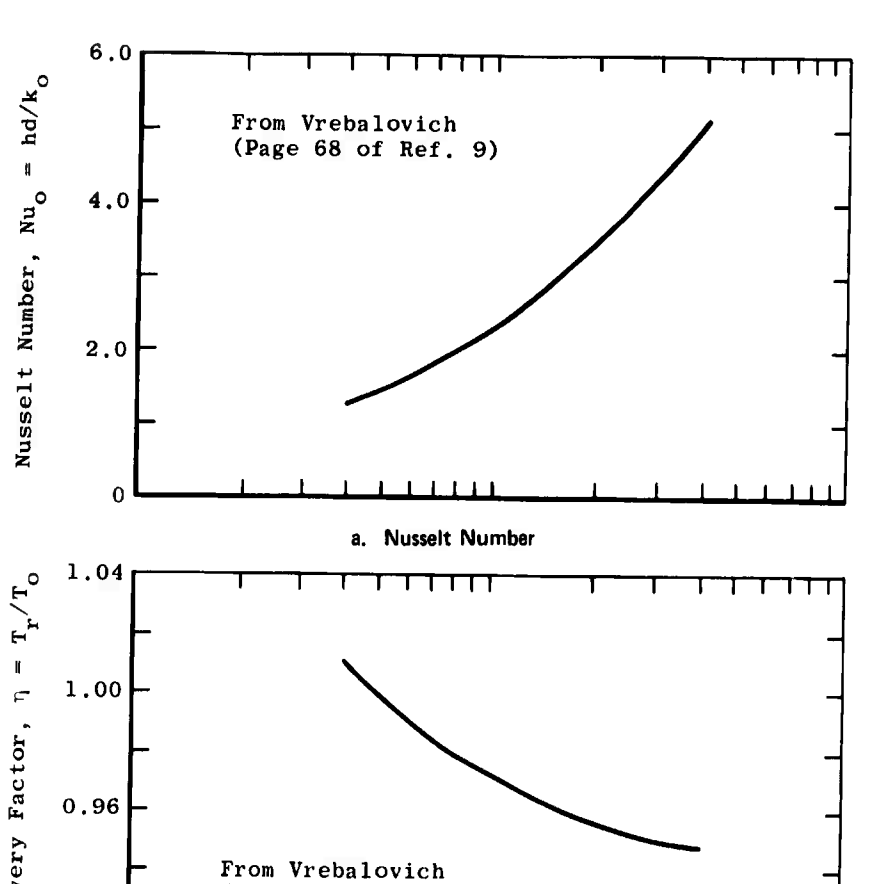

a. Nusselt Number

b. Temperature Recovery Factor

Fig. 5 Hot-Wire Heat-Loss Variation with Unit Reynolds Number, $M_\infty = 4.0$, $d = 10^{-4}$ in., $T_o = 530°R$

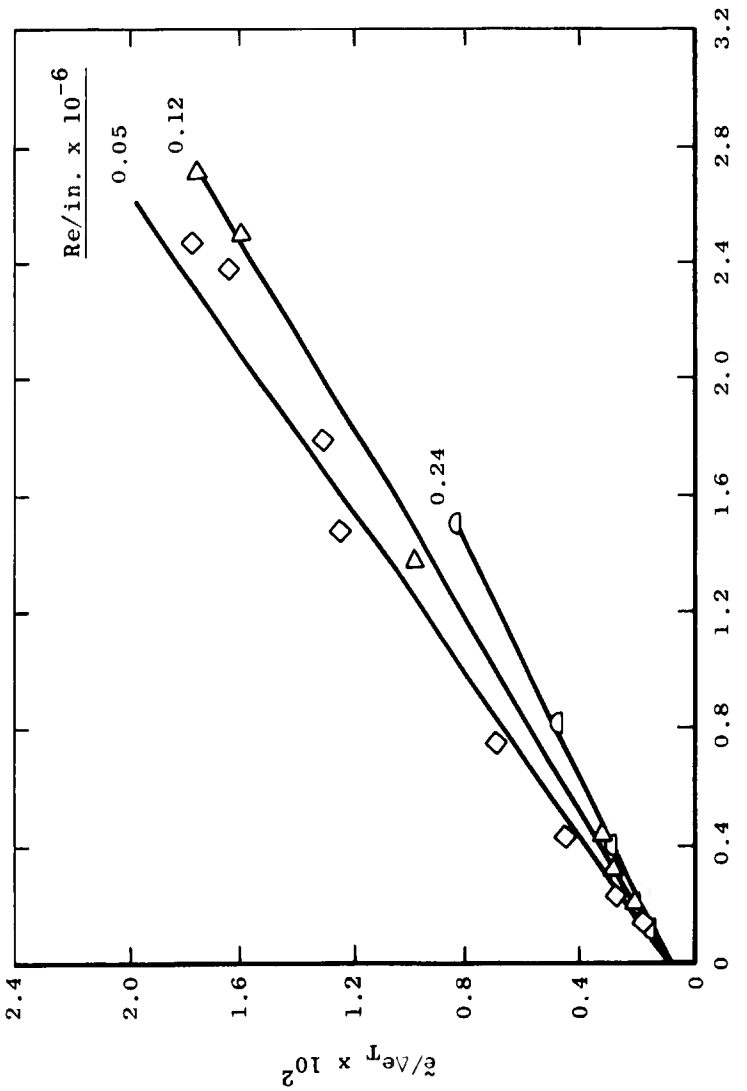

Fig. 6 Mode Diagrams

Notes: 1. Bars indicate data spread possible with alternate fairings of mode diagram for each unit Reynolds number (Fig. 6).

2. Absence of bars indicates data spread is within symbol.

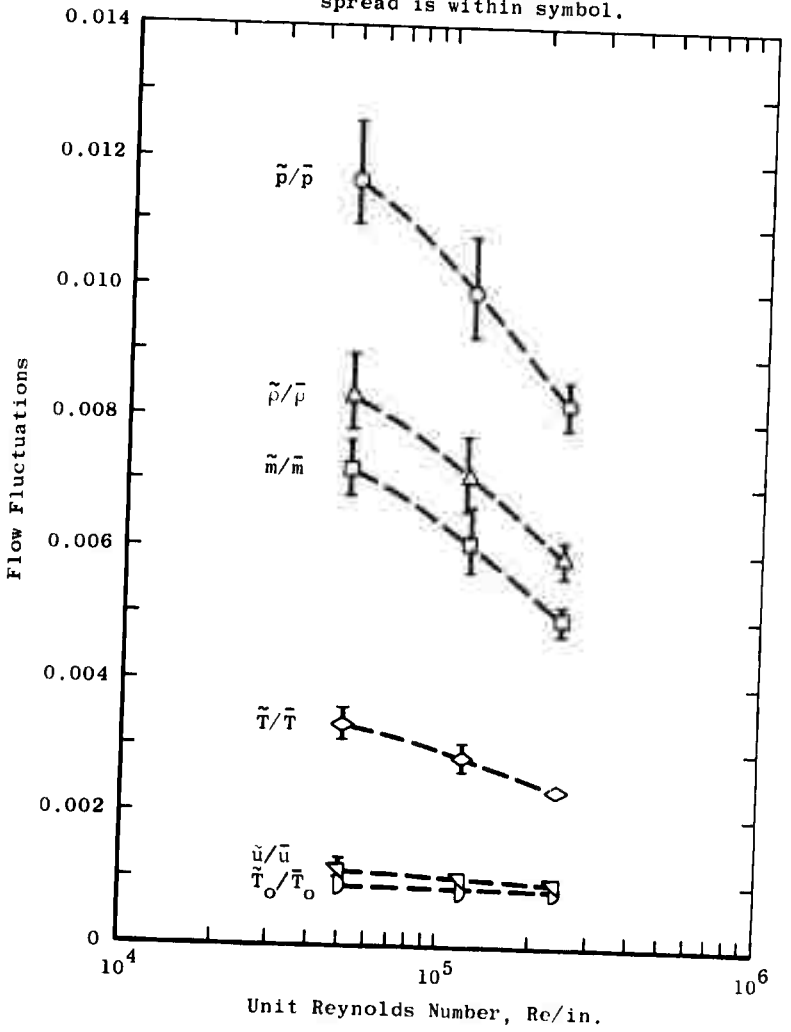

Fig. 7 Variation of Flow Flunctuations with Unit Reynolds Number

Note: Bars in Figs. 8 and 9 indicate data spread possible with alternate fairings of mode diagrams for each unit Reynolds number (Fig. 6).

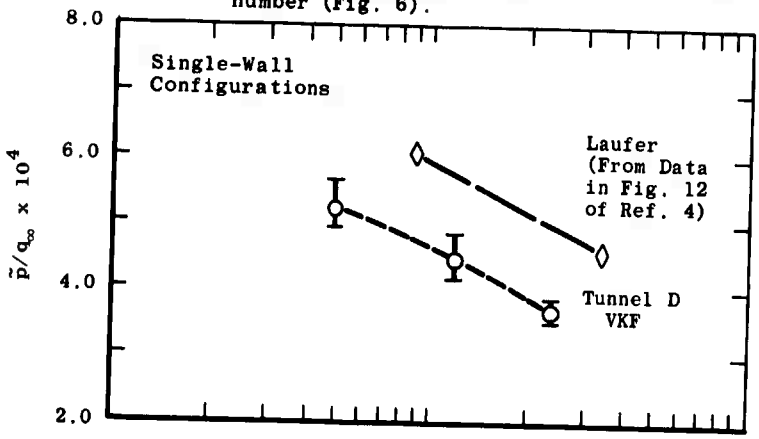

Fig. 8 Variation of RMS Pressure Fluctuations (Normalized by Dynamic Pressure) with Unit Reynolds Number

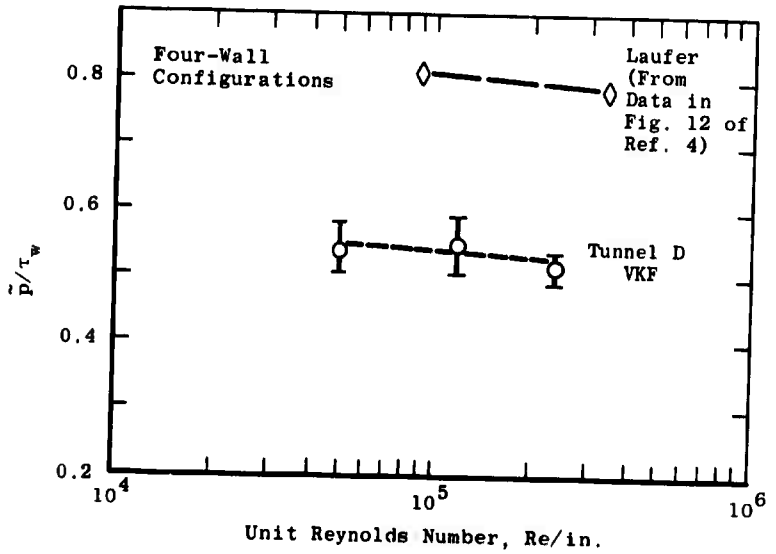

Fig. 9 Variation of RMS Pressure Fluctuations (Normalized by Wall Shearing Stress) with Unit Reynolds Number

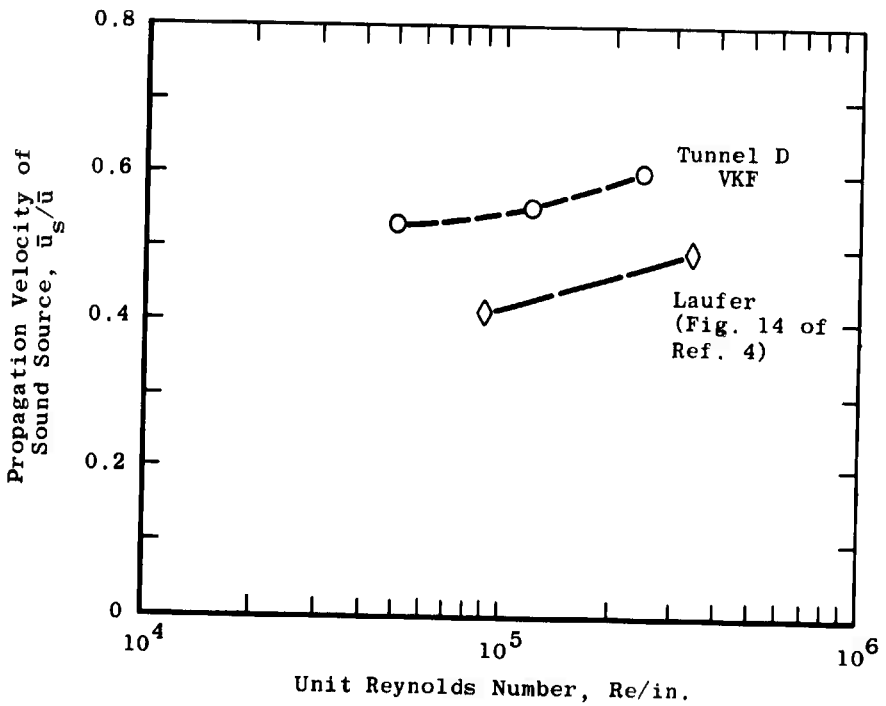

Fig. 10 Variation of Sound–Source Velocity with Unit Reynolds Number

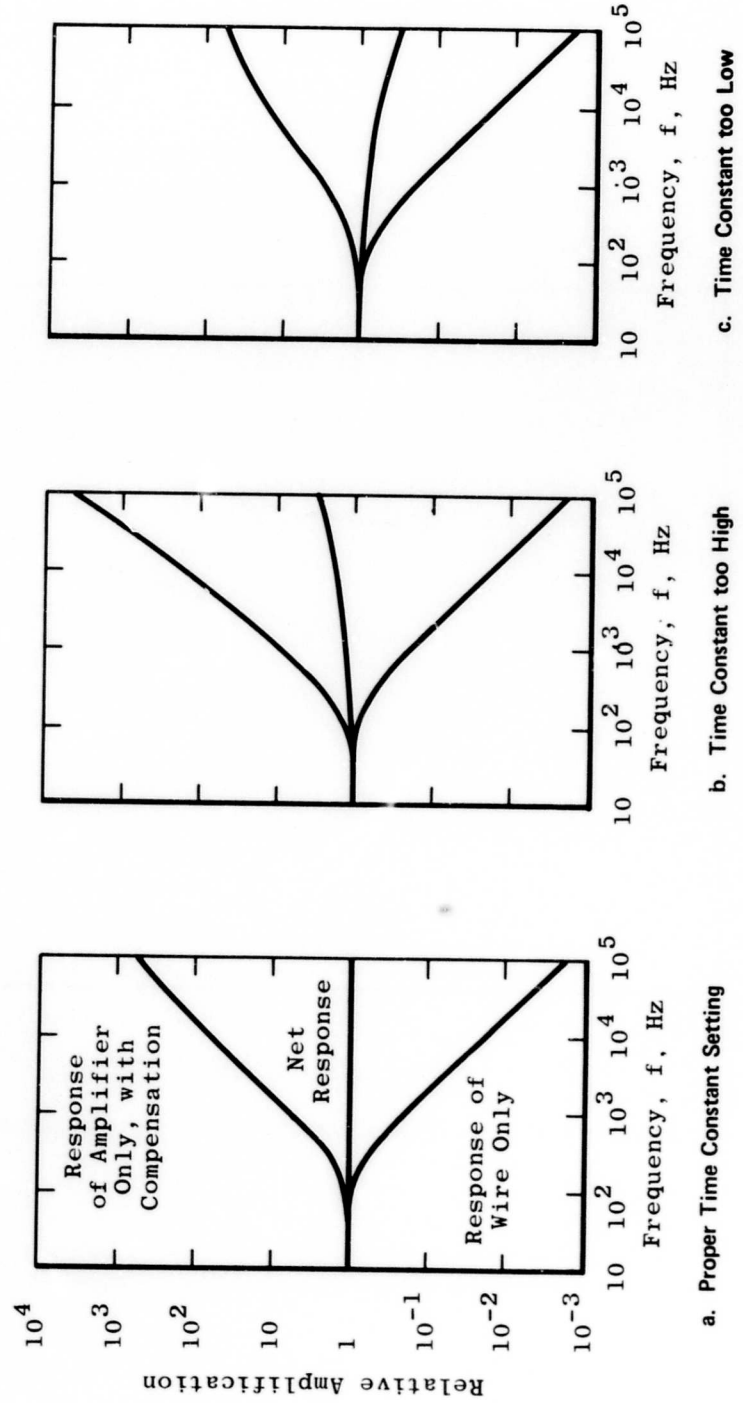

a. Proper Time Constant Setting

b. Time Constant too High

c. Time Constant too Low

Fig. 11 Effects of Time Constant Setting on Anemometer Response

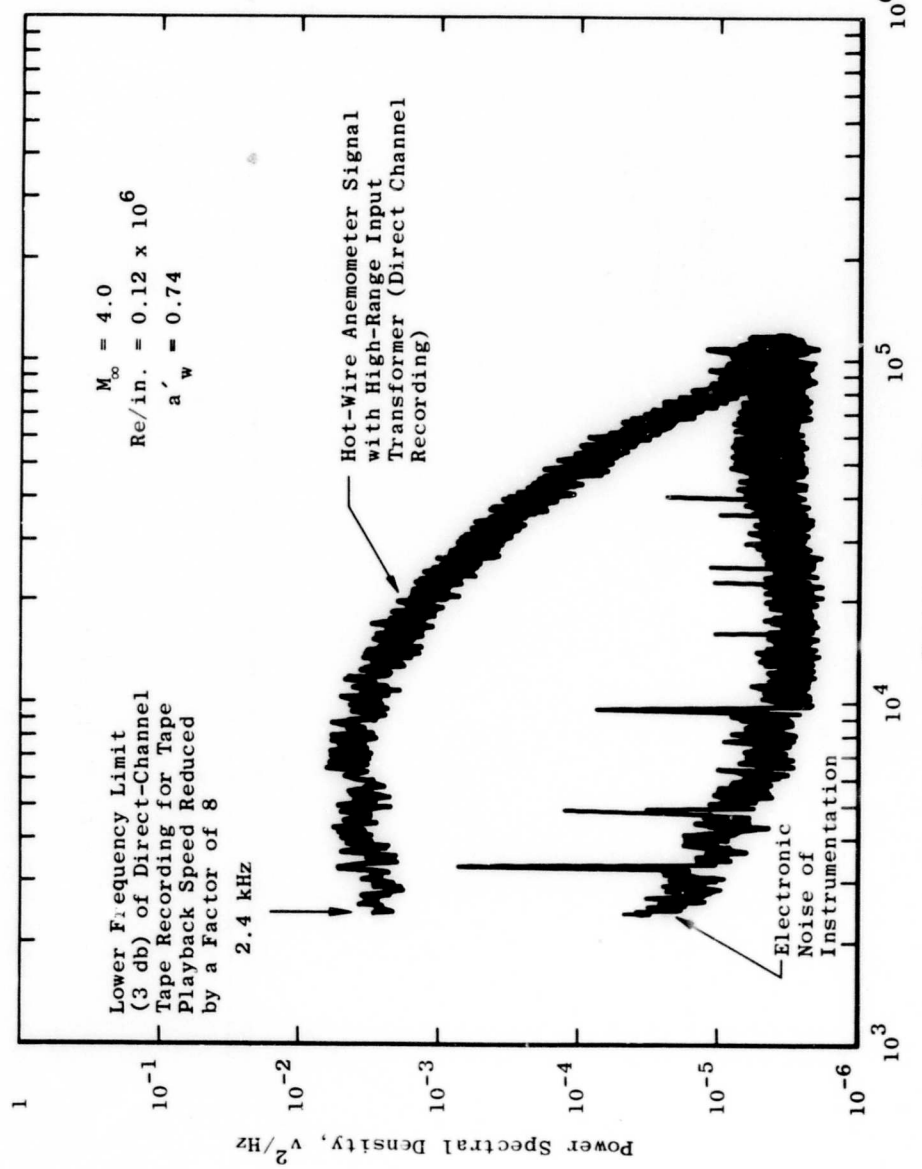

Fig. 12 Typical Hot-Wire Response and Electronic Noise at High Frequencies

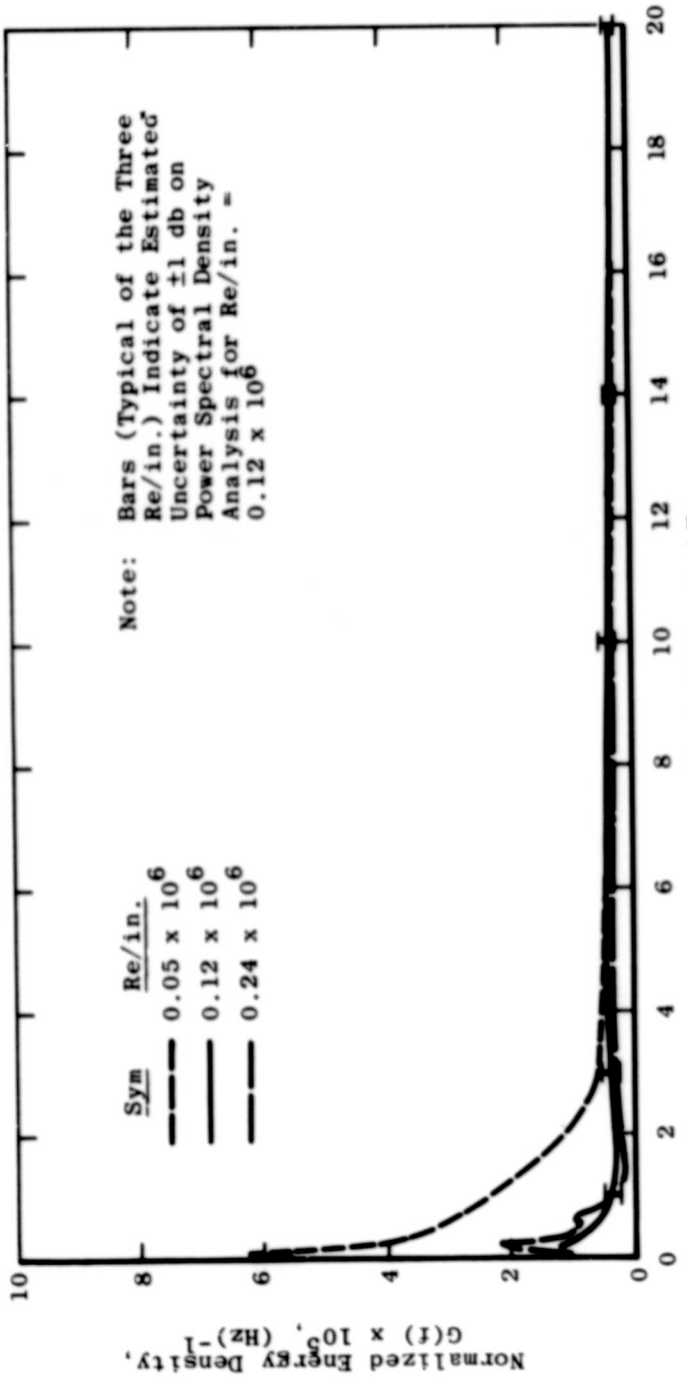

a. $a'_w = 0.05$

Fig. 13 Normalized Energy Density Distribution

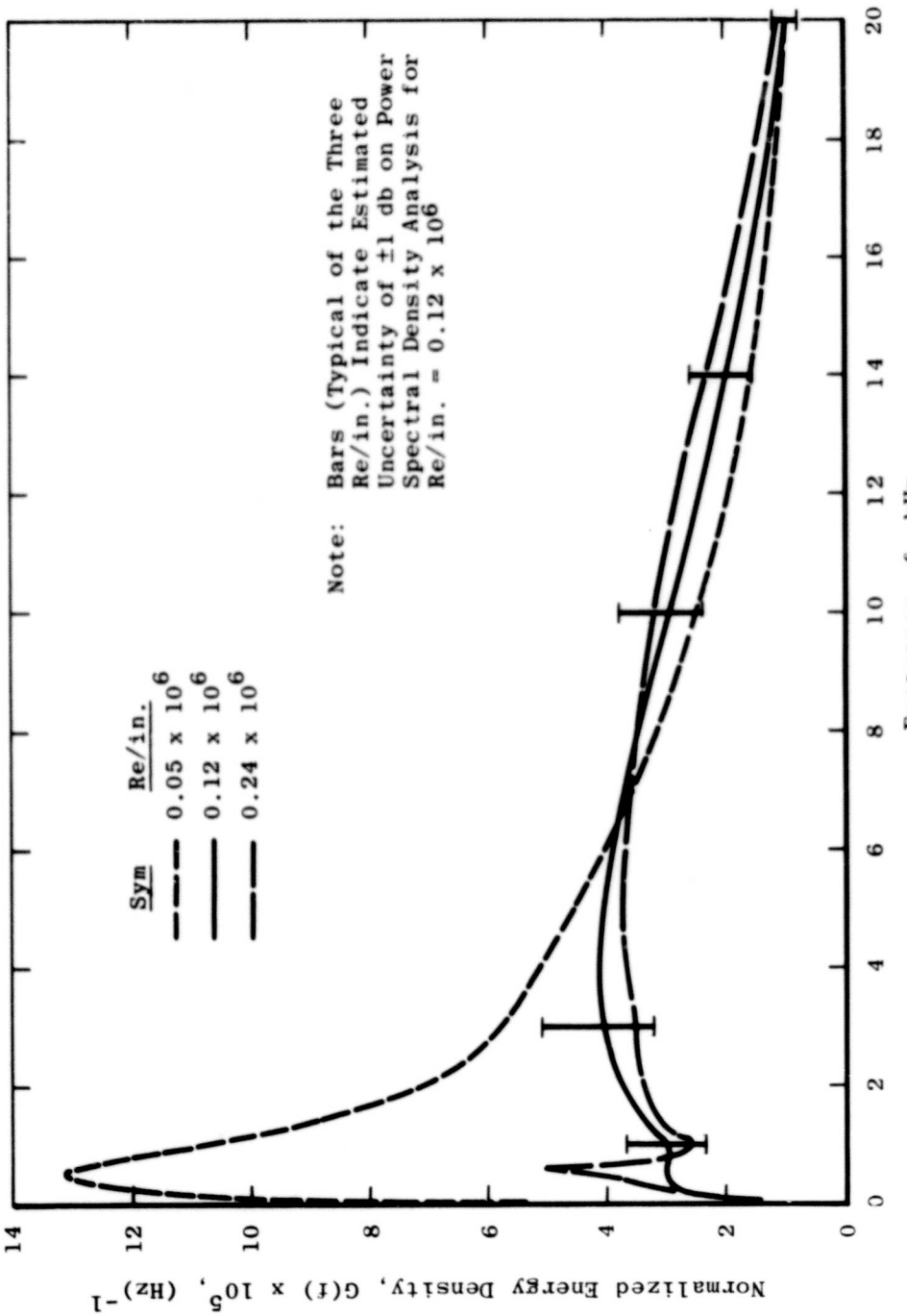

b. $a'_w = 0.4$

Fig. 13 Continued

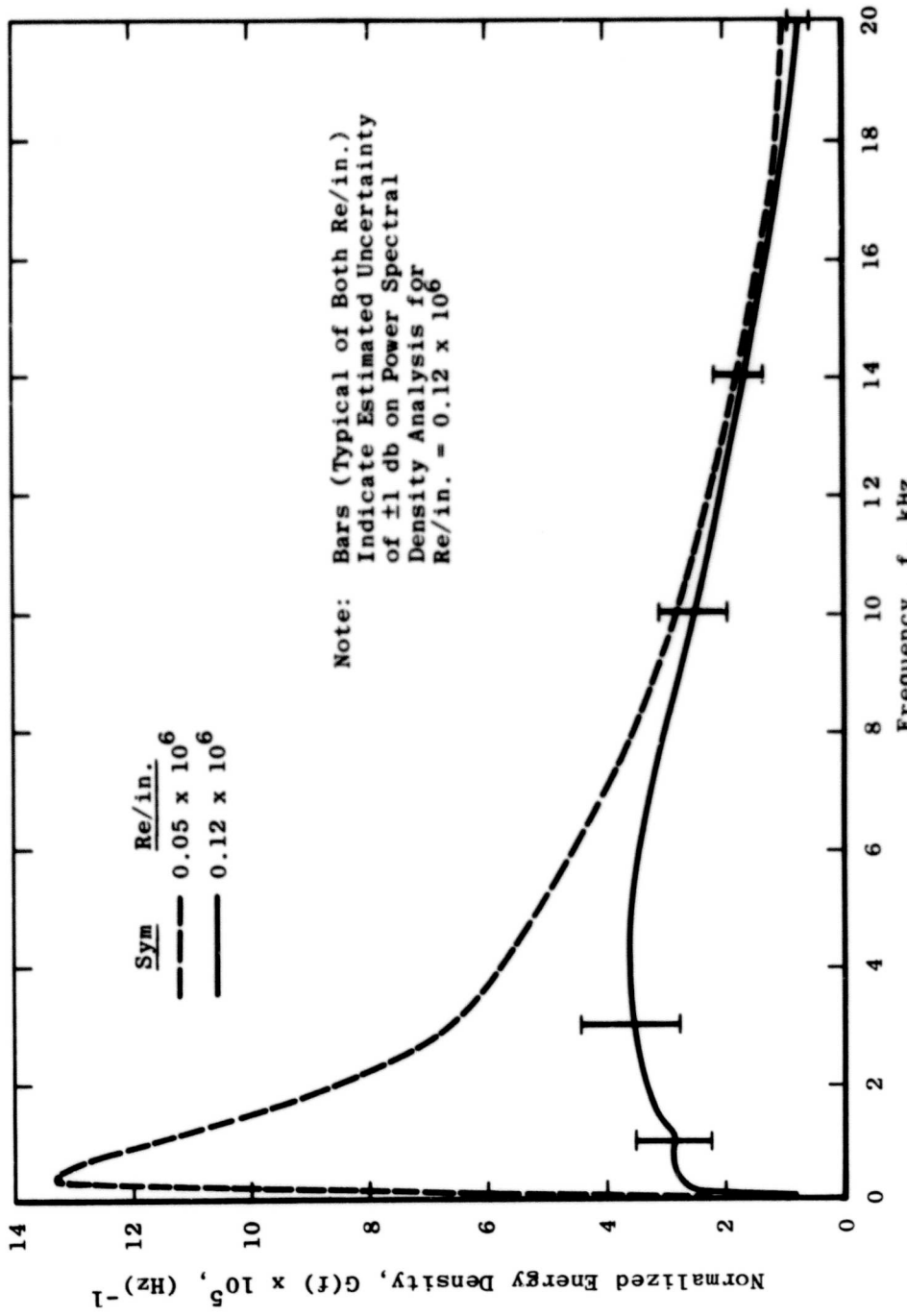

c. $\delta'_w = 0.5$

Fig. 13 Concluded

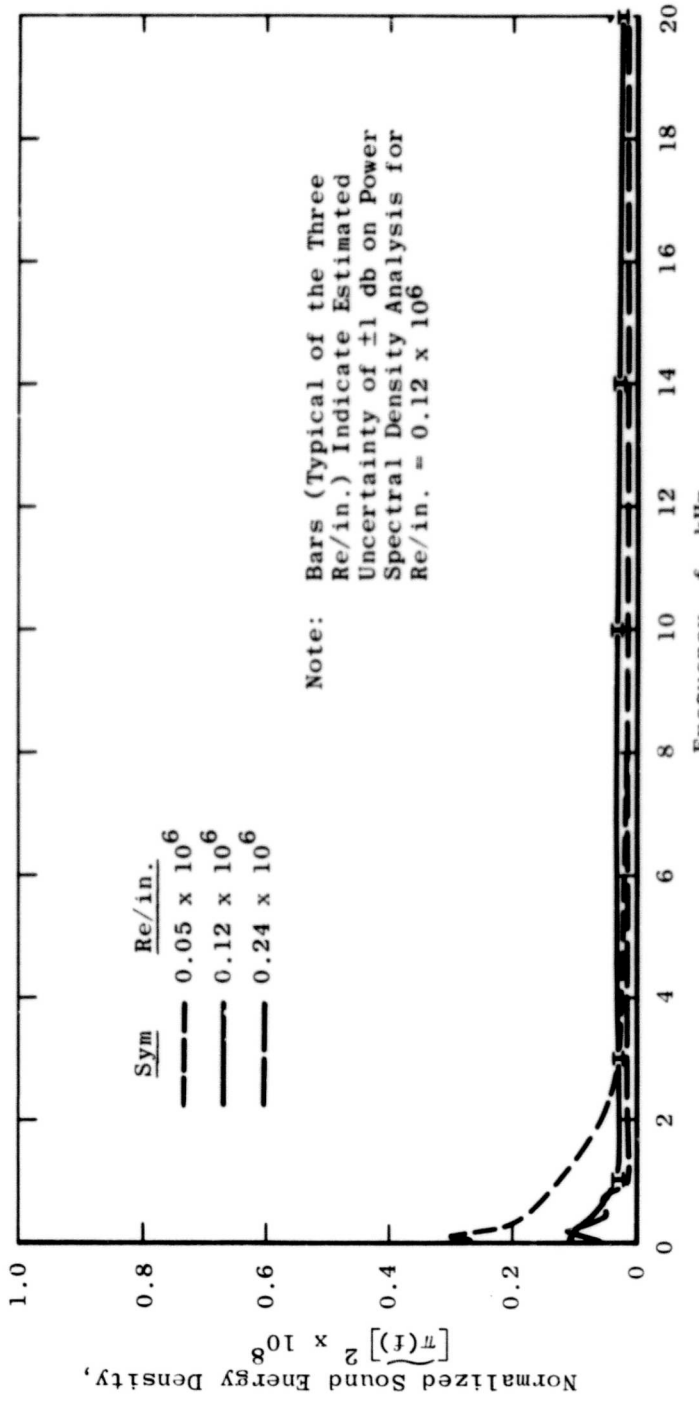

a. $a'_w = 0.05$

Fig. 14 Normalized Sound Energy Density Distribution

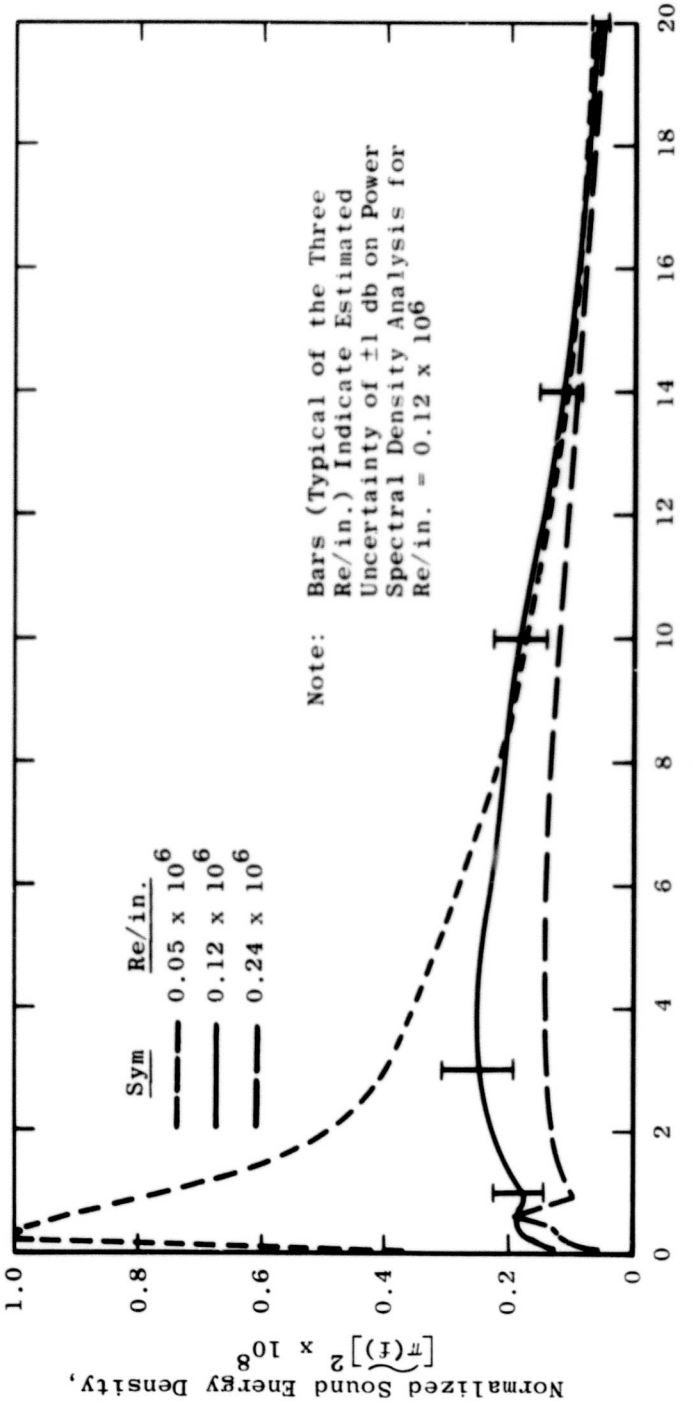

b. $a'_w = 0.4$

Fig. 14 Continued

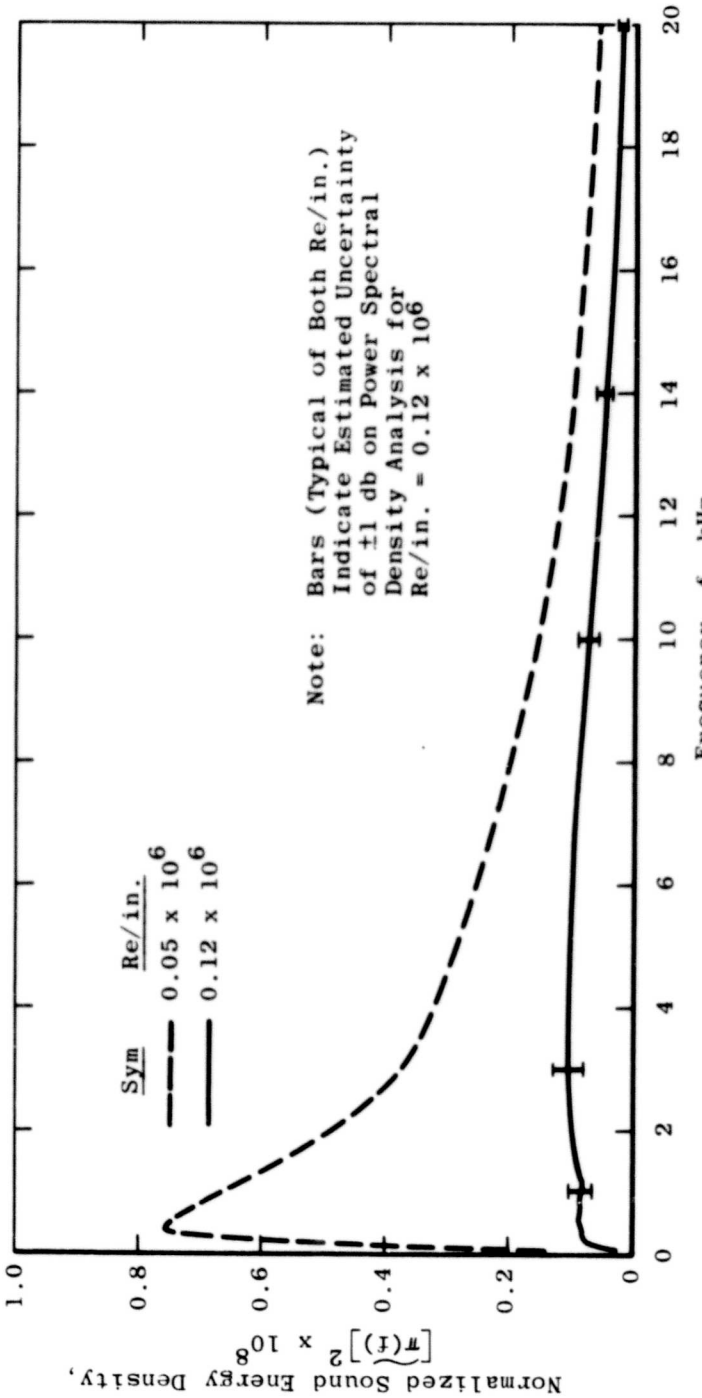

c. $a'_w = 0.5$

Fig. 14 Concluded

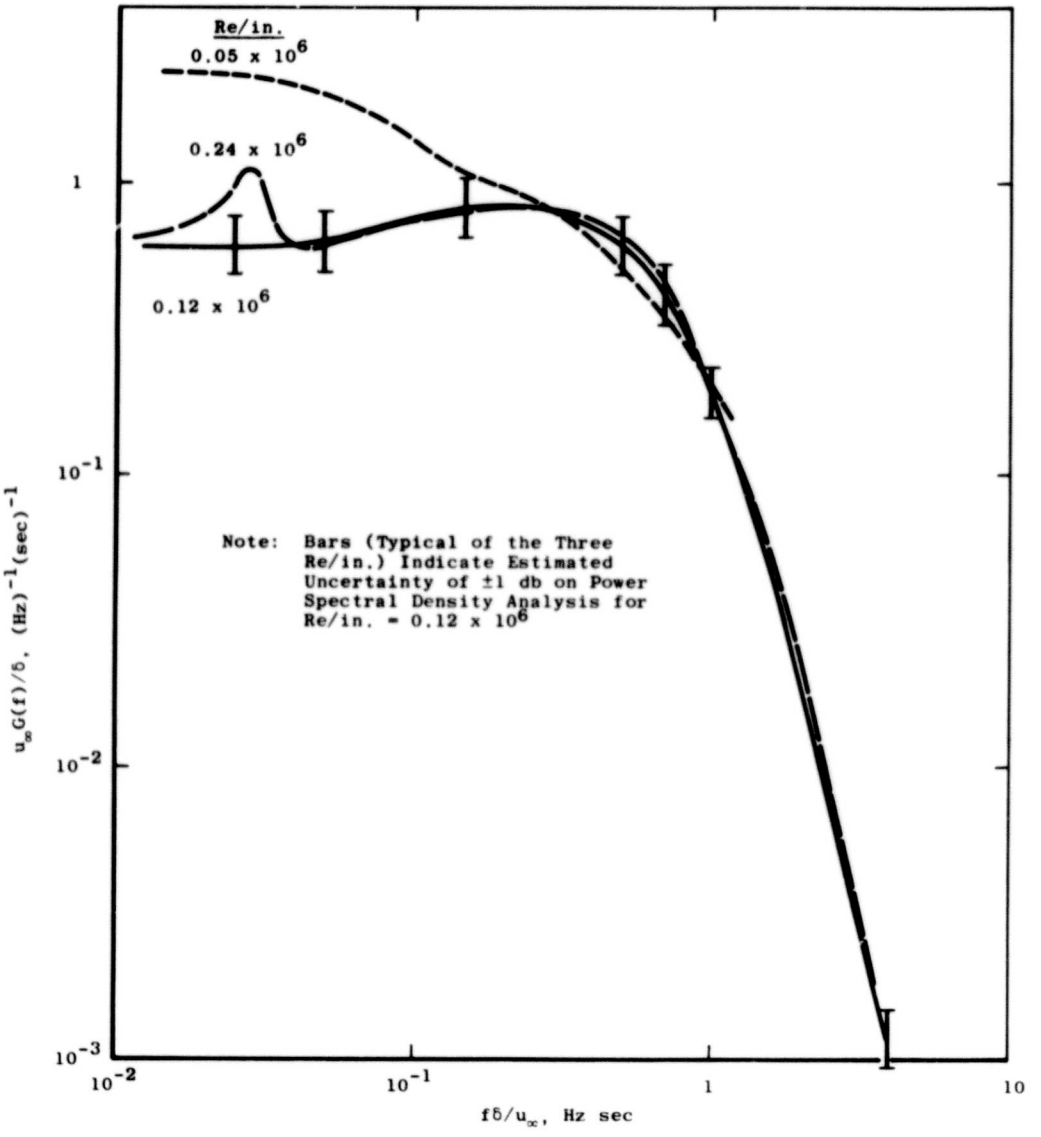

Fig. 15 Hot-Wire Signal Spectra for Wire Overheat of $a'_w = 0.4$

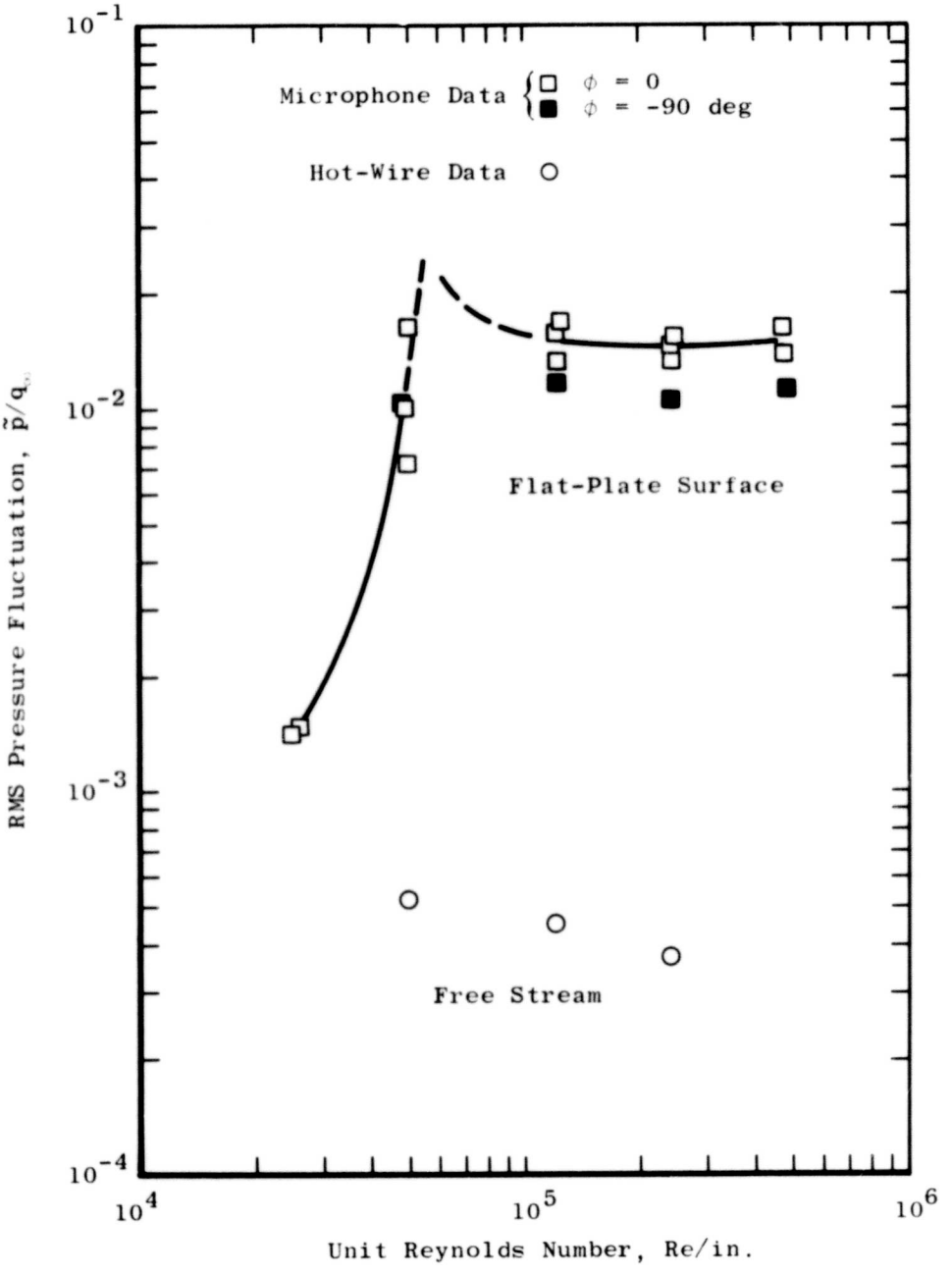

Fig. 16 Comparison of Flat-Plate Surface and Free-Stream Pressure Fluctuations

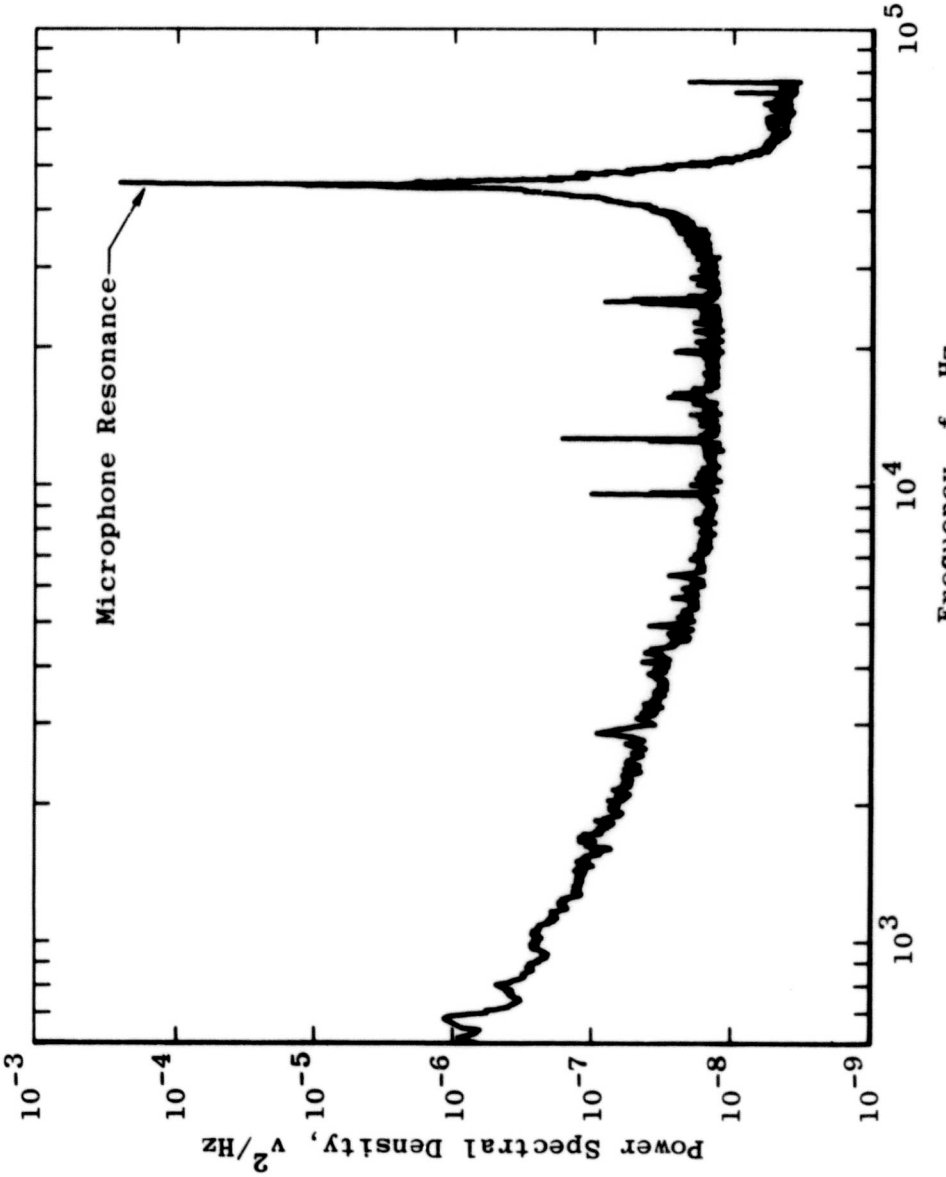

Fig. 17 Power Spectral Density Analysis of Microphone Output Recorded at Re/in. = 0.24 x 10^6

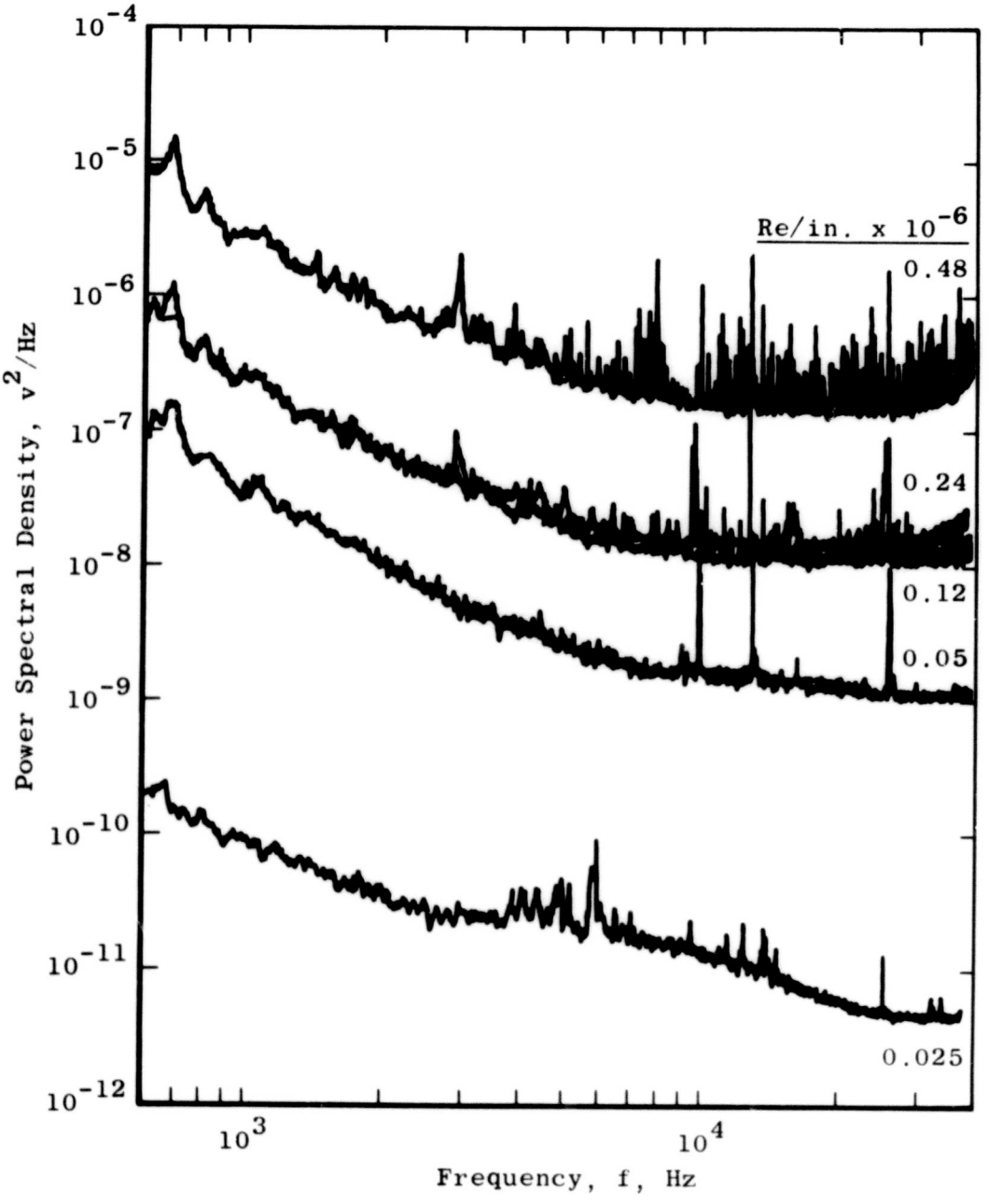

Fig. 18 Comparison of Power Spectra of Microphone Output for Various Unit Reynolds Numbers

TABLE I
MODE SENSITIVITY COEFFICIENTS

$$\Delta e_\tau = \bar{e}\, E' \left[\alpha_M K(\gamma-1)M^2 + \frac{A'_w}{\tau_r} \left\{ \frac{\partial \ell n\, \eta}{\partial \ell n\, M} + \frac{\partial \ell n\, \eta}{\partial \ell n\, Re_o} (1 - 0.765\alpha_M(\gamma-1)M^2) \right\} \right.$$

$$\left. - A'_w \left\{ -(K - 1.885)\, \alpha_M(\gamma-1)M^2 + \frac{\partial \ell n\, Nu_o}{\partial \ell n\, Re_o} (1 - 0.765\alpha_M(\gamma-1)M^2) + \frac{\partial \ell n\, Nu_o}{\partial \ell n\, M} \right\} \right]$$

$$\Delta e_\sigma = \bar{e}\, E' \left[\alpha_M K - \frac{A_w}{\tau_r} \left\{ 0.5 \frac{\partial \ell n\, \eta}{\partial \ell n\, M} + \frac{\partial \ell n\, \eta}{\partial \ell n\, Re_o} (1 + 0.765\alpha_M) \right\} \right.$$

$$\left. + A'_w \left\{ (K - 1.885)\alpha_M + \frac{\partial \ell n\, Nu_o}{\partial \ell n\, Re_o} (1 + 0.765\alpha_M) + 0.5 \frac{\partial \ell n\, Nu_o}{\partial \ell n\, M} \right\} \right]$$

$$\Delta e_\pi = \bar{e}\, E' \left[\alpha_M K(\gamma-1)(1 + n_x M) - \frac{A'_w}{\tau_r} \left\{ \left(\frac{\gamma-1}{2} - \frac{n_x}{M} \right) \frac{\partial \ell n\, \eta}{\partial \ell n\, M} + \frac{\partial \ell n\, \eta}{\partial \ell n\, Re_o} \left[0.765\alpha_M(\gamma-1)(1 + n_x M) - \left(1 + \frac{n_x}{M} \right) \right] \right\} \right.$$

$$\left. + A'_w \left\{ (K - 1.885)\alpha_M (\gamma-1)(1 + n_x M) \right.\right.$$

$$\left.\left. + \frac{\partial \ell n\, Nu_o}{\partial \ell n\, Re_o} \left[0.765\alpha_M (\gamma-1)(1 + n_x M) - \left(1 + \frac{n_x}{M} \right) \right] + \frac{\partial \ell n\, Nu_o}{\partial \ell n\, M} \left(\frac{\gamma-1}{2} - \frac{n_x}{M} \right) \right\} \right]$$